BENNETT

AI-POWERED BIOLOGICAL INTELLIGENCE

IDENTIFYN RESOLUTION STEPDOWN

ATM.P

MICROSCOPY EVIDENCE ASSESSMENT

Rabbit anti-Human ATM.p (Serine 1981) Recombinant Monoclonal

WESTERN BLOT -> WIDEFIELD -> WIDEFIELD SIM / APOTOME -> CONFOCAL -> AIRYSCAN
SIM -> SIM² -> SINGLE-MOLECULE STORM

8	1	PENDING
ORDERED EVIDENCE TIERS	SUPPORTING CONTROL	SCIENTIST REVIEW

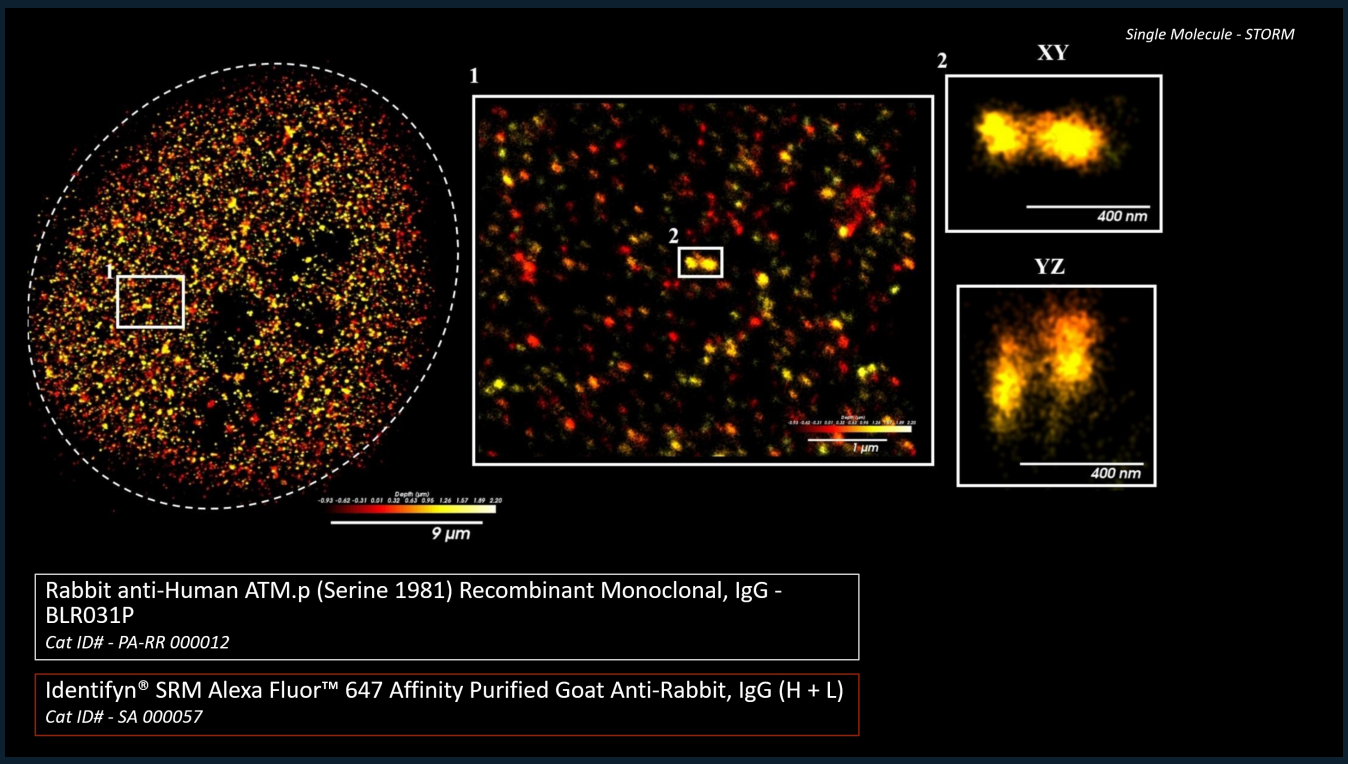

Rabbit anti-Human ATM.p (Serine 1981) Recombinant Monoclonal, IgG - BLR031P
Cat ID# - PA-RR 000012

Identifyn® SRM Alexa Fluor™ 647 Affinity Purified Goat Anti-Rabbit, IgG (H + L)
Cat ID# - SA 000057

REPRESENTATIVE HIGHEST-AVAILABLE VIEW / SINGLE-MOLECULE STORM

PA-RR-000012 | PRODUCT-LEVEL EVIDENCE DOSSIER

SOURCE-GROUNDED MICROSCOPY + BIOLOGICAL REVIEW / IDENTIFYN EVIDENCE PRESERVED

CRO CAPABILITY DEMONSTRATED

Identifyn performed the experimental and imaging work documented below. BENNETT converts that operating history into a governed, source-bounded scientific record.

- Source-documented sample preparation and antibody/reagent workflow
- Western blot imaging
- Widefield fluorescence microscopy
- Widefield structured illumination / Apotome optical sectioning
- Confocal microscopy
- Airyscan acquisition and reconstruction workflow
- Structured illumination microscopy
- SIM² reconstruction workflow
- Single-molecule STORM presentation workflow
- Preserved control experiment
- Treatment-response experimental workflow
- Z-stack / 3D acquisition
- Multi-channel imaging

SCIENTIFIC QUESTION

What source-bounded experimental and microscopy evidence is preserved for ATM.p, and what is the strongest interpretation allowed by the available modalities and controls?

EVIDENCE AVAILABLE

Western blot -> Widefield -> Widefield SIM — Apotome -> Confocal -> Airyscan -> SIM -> SIM² -> Single-molecule STORM -> Control

BENNETT ASSESSMENT

The preserved PA-RR-000012 record contains the full ordered evidence sequence from Western blot through single-molecule STORM. Each modality retains its own acquisition and processing boundary.

BENNETT / MICROSCOPY AND BIOLOGICAL EVIDENCE REVIEW

SOURCE-GROUNDED RETROSPECTIVE REVIEW / PENDING SCIENTIST REVIEW

SOURCE STATE	SOURCE HASH VERIFIED / EVENT RECORDED
BENNETT EVIDENCE REVIEW	COMPLETED / SOURCE-BOUNDED
NATIVE IMAGE REPROCESSING	NOT PERFORMED
LITERATURE SOURCES	INDEPENDENTLY VERIFIED
SCIENTIST REVIEW	PENDING
PUBLICATION	NOT AUTHORIZED

OVERALL CALL / FULL STEPDOWN / SOURCE-BOUNDED REVIEW

The preserved PA-RR-000012 record contains the full ordered evidence sequence from Western blot through single-molecule STORM. Each modality retains its own acquisition and processing boundary.

SETTINGS ASSESSMENT

The record preserves 8 ordered evidence tier(s). Structured source metadata values are reported by stage and remain tied to the original method objects.

BIOLOGICAL SUPPORT

The record supports retrospective, source-bounded microscopy review. Target identity, specificity, treatment effect, binding, interaction and mechanism are not inferred from presentation images alone.

CONTROL ASSESSMENT

A true preserved control record is present and appears last.

CLAIM CEILING

This draft supports historical capability documentation, source registration, modality ordering, settings review and bounded interpretation. It does not independently validate antibody specificity, quantify a population response, establish binding, interaction, causation or mechanism, or authorize publication.

PROCESSING DISCLOSURE

Retrospective BENNETT architectural evaluation of preserved Identifyn source evidence. BENNETT did not perform native-file reprocessing, new deterministic measurement or the historical image post-processing represented in this record.

REAGENTS AND ACQUIRED CHANNELS

Preparation reagents are reported separately from channels actually documented in the acquisition settings. Fluorophores mentioned in staining are not automatically treated as acquired channels.

EVIDENCE OBJECT	REAGENTS / FLUOROPHORES PRESENT	CHANNELS ACTUALLY ACQUIRED
Western blot	647	Not deterministically stated in the acquisition block
Widefield	405/DAPI; 488; 647; 680	3; 50 Cy 5; 38 eGFP; 49 DAPI; 625 - 655; 450 - 490; 335 - 383; 665 - 715
Widefield SIM — Apotome	405/DAPI; 488; 647	2; 50 Cy 5; 38 HE eGFP; 625 - 655; 450 - 490; 665 - 715; 500 - 550; 653
Confocal	405/DAPI; 488; 647	2; None; 639 nm @ 0.3%; 488 nm @ 0.3%; 653; 493; 668; 517
Airyscan	405/DAPI; 488; 647	2; None; 639 nm @ 0.40%; 488 nm @ 0.5%; 653; 493; 668; 517
SIM	405/DAPI; 488; 647	2; SR HE LBF 405/488/561/642; 200 - 405, 200 - 488, 200 - 561, 200 - 642; 419 - 470, 503 - 546, 576 - 617, 657 - 800; T1-Axiocam 820; T2-Axiocam 820; 640; 488
SIM²	405/DAPI; 488; 647	2; SR HE LBF 405/488/561/642; 200 - 405, 200 - 488, 200 - 561, 200 - 642; 419 - 470, 503 - 546, 576 - 617, 657 - 800; T1-Axiocam 820 -SR; T2-Axiocam 820-SR; 640; 488
Single-molecule STORM	647	Both Channels
Control	405/DAPI; 488; 647	1; None; 639 nm @ 0.3%; 653; 668

MODALITY ASSESSMENT / PART 1 OF 9

Western blot / SOURCE EVIDENCE PRESERVED

DOCUMENTED SETTINGS

Platform: Azure Sapphire FL. Objective: not explicitly stated. Platform: Azure Sapphire FL with Customizable Laser and Filter Modules, Enabling UV-NIR and Z-Plane Imaging.. Structured source metadata values: 11.

VISIBLE OBSERVATION

A preserved presentation image is available for Western blot. BENNETT records the visible source presentation without creating a new native measurement.

SOURCE-REPORTED RESULT

The source identifies this object as Western blot, documents platform context as Azure Sapphire FL, and records detected dye/channel descriptors as 647.

LITERATURE CORRELATION

Consistent with peer-reviewed microscopy and antibody-validation guidance that presentation evidence must remain bounded by modality, controls and source documentation.

INTERPRETIVE LIMIT

Band position and displayed intensity do not independently establish analytical specificity, target identity, linearity, or treatment effect.

CLAIM CEILING

This tier supports a source-bounded statement that the historical Western blot evidence and documented settings are preserved for review; stronger biological or quantitative conclusions require compatible native data, controls and scientist review.

MODALITY ASSESSMENT / PART 2 OF 9

Widefield / SOURCE EVIDENCE PRESERVED

DOCUMENTED SETTINGS

Platform: ZEISS Axio Imager.M1. Objective: Plan-Apochromat 63x/1.40 Oil M27. Platform: Zeiss Axio Imager.M1 Widefield, using a Plan-Apochromat 63x/1.40 Oil M27, Axiocam 705, and X-Cite Xylis Lamp, was used with the following parameters for each dye:. Acquisition: Channels: 3; Scaling (Per Pixel): 0.110 µm X 0.110 µm; Image size (Pixels): 680 X 559; Image Size (Pixels): 680 X 559; Bit Depth: 14 Bit. Detector/camera: Imaging Device: Axiocam 705. Timing: Exposure Time: 150 ms; 30 ms. Illumination: Light source: X-Cite Xylis Lamp Intensity @ 15.00%; X-Cite Xylis Lamp Intensity @ 10.00%. Optical/scan: Effective NA: 1.4. Structured source metadata values: 38.

VISIBLE OBSERVATION

A preserved presentation image is available for Widefield. BENNETT records the visible source presentation without creating a new native measurement.

SOURCE-REPORTED RESULT

The source identifies this object as Widefield, documents platform context as ZEISS Axio Imager.M1, and records detected dye/channel descriptors as 405/DAPI; 488; 647; 680.

LITERATURE CORRELATION

Consistent with peer-reviewed microscopy and antibody-validation guidance that presentation evidence must remain bounded by modality, controls and source documentation.

INTERPRETIVE LIMIT

A presentation image supports gross localization and source-bounded co-occurrence, not direct binding, molecular colocalization, or native quantitative measurement.

CLAIM CEILING

This tier supports a source-bounded statement that the historical Widefield evidence and documented settings are preserved for review; stronger biological or quantitative conclusions require compatible native data, controls and scientist review.

MODALITY ASSESSMENT / PART 3 OF 9

Widefield SIM — Apotome / SOURCE EVIDENCE PRESERVED

DOCUMENTED SETTINGS

Platform: ZEISS Axio Observer.Z1/7 Apotome. Objective: EC Plan-Neofluar 63x/1.25 Oil M27. Platform: Zeiss Axio Observer.Z1/7 Apotome SIM, using an EC Plan-Neofluar 63x/1.25 Oil M27, Axiocam 807 Mono, and X-Cite Xylis Lamp was used with the following parameters for each dye:. Acquisition: Z-Stack: 78 Slices (7.7 µm); Channels: 2; Scaling (Per Pixel): 0.143 µm X 0.143 µm X 0.100 µm; Image size (Pixels): 864 X 791; 324 X 317; Image Size (Pixels): 864 X 791; 324 X 317; Bit Depth: 14 Bit. Detector/camera: Imaging Device: Axiocam 807 Mono. Timing: Exposure Time: 100 ms; 250 ms. Illumination: Light source: X-Cite Xylis Lamp Intensity @ 10.00%; X-Cite Xylis Lamp Intensity @ 25.00%. Optical/scan: Effective NA: 1.25. Processing: Projection: View Angle 35°, Scale Z 100%, Reverse Z-Axis NOT Selected, Stereo Anaglyph NOT Selected, Camera Separation 5% (deselected), Parallax Shift 0% (deselected); Background: Black. Structured source metadata values: 50.

VISIBLE OBSERVATION

A preserved presentation image is available for Widefield SIM — Apotome. BENNETT records the visible source presentation without creating a new native measurement.

SOURCE-REPORTED RESULT

The source identifies this object as Widefield SIM — Apotome, documents platform context as ZEISS Axio Observer.Z1/7 Apotome, and records detected dye/channel descriptors as 405/DAPI; 488; 647.

LITERATURE CORRELATION

Consistent with peer-reviewed microscopy and antibody-validation guidance that presentation evidence must remain bounded by modality, controls and source documentation.

INTERPRETIVE LIMIT

Improved optical sectioning does not by itself establish reconstructed super-resolution or molecular interaction.

CLAIM CEILING

This tier supports a source-bounded statement that the historical Widefield SIM — Apotome evidence and documented settings are preserved for review; stronger biological or quantitative conclusions require compatible native data, controls and scientist review.

MODALITY ASSESSMENT / PART 4 OF 9

Confocal / SOURCE EVIDENCE PRESERVED

DOCUMENTED SETTINGS

Platform: ZEISS LSM 980. Objective: Plan-Apochromat 63x/1.40 Oil DIC M27. Platform: Zeiss LSM980 Confocal with NIR Detection, Axio Observer.Z1/7, using a Plan-Apochromat 63x/1.40 Oil DIC M27, was used with the following parameters for each dye:. Acquisition: Z-Stack: 73 Slices (2.16 µm); Channels: 2; Scaling (Per Pixel): 0.059 µm X 0.059 µm X 0.030 µm; Image size (Pixels): 1341 X 1115; Image Size (Pixels): 1341 X 1115; Bit Depth: 16 Bit. Detector/camera: Imaging Device: GaAsP-Pmt3; Detector Type: GaAsP-PMT. Timing: Pixel Time: 0.26 µs; Frame Time: 5.63 s. Illumination: Laser Wavelength: 639 nm @ 0.3%; 488 nm @ 0.3%. Optical/scan: Pinhole: 1.00 AU / 65 µm; 1.00 AU / 51 µm; Scan Zoom: 1.5; LSM Scan Speed: 11; Scan Direction: Bidirectional; Averaging: 8; Effective NA: 1.4. Processing: LSM Plus Mode: Filter: 8.1 (3D, Auto); Filter: 7.7 (3D, Auto). Structured source metadata values: 46.

VISIBLE OBSERVATION

A preserved presentation image is available for Confocal. BENNETT records the visible source presentation without creating a new native measurement.

SOURCE-REPORTED RESULT

The source identifies this object as Confocal, documents platform context as ZEISS LSM 980, and records detected dye/channel descriptors as 405/DAPI; 488; 647.

LITERATURE CORRELATION

Consistent with peer-reviewed microscopy and antibody-validation guidance that presentation evidence must remain bounded by modality, controls and source documentation.

INTERPRETIVE LIMIT

Optical sectioning and source-bounded 3D presentation do not establish binding, mechanism, or population-level effect.

CLAIM CEILING

This tier supports a source-bounded statement that the historical Confocal evidence and documented settings are preserved for review; stronger biological or quantitative conclusions require compatible native data, controls and scientist review.

MODALITY ASSESSMENT / PART 5 OF 9

Airyscan / SOURCE EVIDENCE PRESERVED

DOCUMENTED SETTINGS

Platform: ZEISS LSM 980. Objective: Plan-Apochromat 63x/1.40 Oil DIC M27. Platform: Zeiss LSM980 Confocal with NIR Detection, Axio Observer.Z1/7, using a Plan-Apochromat 63x/1.40 Oil DIC M27, was used with the following parameters for each dye:. Acquisition: Z-Stack: 82 Slices (2.43 µm); Channels: 2; Scaling (Per Pixel): 35.29 nm X 35.29 nm X 30.00 nm; Image size (Pixels): 945 X 703; 154 X 118; Image Size (Pixels): 945 X 703; 154 X 118; Bit Depth: 16 Bit. Detector/camera: Imaging Device: Airyscan; Detector Type: GaAsP-PMT. Timing: Pixel Time: 1.04 µs; Frame Time: 19.77 s. Illumination: Laser Wavelength: 639 nm @ 0.40%; 488 nm @ 0.5%. Optical/scan: Pinhole: 5.00 AU / 328 µm; 5.00 AU / 250 µm; Scan Zoom: 1.9; LSM Scan Speed: 6; Scan Direction: Bidirectional; Averaging: 4; Effective NA: 1.4. Processing: AiryScan Mode: Super Resolution: 9.8 (3D, Auto); Super Resolution: 9.5 (3D, Auto). Structured source metadata values: 46.

VISIBLE OBSERVATION

A preserved presentation image is available for Airyscan. BENNETT records the visible source presentation without creating a new native measurement.

SOURCE-REPORTED RESULT

The source identifies this object as Airyscan, documents platform context as ZEISS LSM 980, and records detected dye/channel descriptors as 405/DAPI; 488; 647.

LITERATURE CORRELATION

Consistent with peer-reviewed microscopy guidance that advanced-resolution outputs remain dependent on acquisition, reconstruction or localization quality control.

INTERPRETIVE LIMIT

Displayed feature separation remains reconstruction dependent; no unsupported numerical resolution or molecular architecture claim is permitted.

CLAIM CEILING

This tier supports a source-bounded statement that the historical Airyscan evidence and documented settings are preserved for review; stronger biological or quantitative conclusions require compatible native data, controls and scientist review.

MODALITY ASSESSMENT / PART 6 OF 9

SIM / SOURCE EVIDENCE PRESERVED

DOCUMENTED SETTINGS

Platform: ZEISS Elyra. Objective: Plan-Apochromat 63X/1.40 oil DIC M27. Platform: Zeiss Elyra 5 Lattice SIM, AxioObserver.Z1/ 7 using Plan-Apochromat 63X/1.40 oil DIC M27, 1X Tubelens, was used with the following parameters for each dye:. Acquisition: Z-Stack: 95 Slices (2.82 µm); Channels: 2; Scaling (Per Pixel): 21.11 nm X 21.11 nm X 30.00 nm; Image size (Pixels): 3155 X 2512; 365 X 360; Image Size (Pixels): 3155 X 2512; 365 X 360; Bit Depth: 16 Bit. Detector/camera: Imaging Device: Axiocam 820. Timing: Exposure Time: 100 ms; 120 ms; Frame Time: 1.33 s; 1.59 s. Illumination: Laser Wavelength: 640 nm @ 1.0%; 488 nm @ 1.00%; Illumination Wavelength: 640; 488. Optical/scan: Scan Direction: Unidirectional; Effective NA: 1.4. Processing: Algorithm: SIM; Process Sampling: N/A; Result Sampling: 4. Structured source metadata values: 50.

VISIBLE OBSERVATION

A preserved presentation image is available for SIM. BENNETT records the visible source presentation without creating a new native measurement.

SOURCE-REPORTED RESULT

The source identifies this object as SIM, documents platform context as ZEISS Elyra, and records detected dye/channel descriptors as 405/DAPI; 488; 647.

LITERATURE CORRELATION

Consistent with peer-reviewed microscopy guidance that advanced-resolution outputs remain dependent on acquisition, reconstruction or localization quality control.

INTERPRETIVE LIMIT

Reconstruction-dependent structural separation requires native reconstruction QC before numerical resolution or molecular dimensions can be claimed.

CLAIM CEILING

This tier supports a source-bounded statement that the historical SIM evidence and documented settings are preserved for review; stronger biological or quantitative conclusions require compatible native data, controls and scientist review.

MODALITY ASSESSMENT / PART 7 OF 9

SIM² / SOURCE EVIDENCE PRESERVED

DOCUMENTED SETTINGS

Platform: ZEISS Elyra. Objective: Plan-Apochromat 63X/1.40 oil DIC M27. Platform: Zeiss Elyra 5 Lattice SIM, AxioObserver.Z1/ 7 using Plan-Apochromat 63X/1.40 oil DIC M27, 1X Tubelens, was used with the following parameters for each dye:. Acquisition: Z-Stack: 120 Slices (3.57 µm); Channels: 2; Scaling (Per Pixel): 21.11 nm X 21.11 nm X 30.00 nm; Image size (Pixels): 1557 X 1805; 376 X 330; Image Size (Pixels): 1557 X 1805; 376 X 330; Bit Depth: 16 Bit. Detector/camera: Imaging Device: Axiocam 820. Timing: Exposure Time: 100 ms; 120 ms; Frame Time: 1.33 s; 1.59 s. Illumination: Laser Wavelength: 640 nm @ 1.0%; 488 nm @ 1.00%; Illumination Wavelength: 640; 488. Optical/scan: Scan Direction: Unidirectional; Effective NA: 1.4. Processing: Algorithm: SIM2; Process Sampling: 4; Result Sampling: 4; Projection: View Angle 45°, Scale Z 35%, Reverse Z-Axis NOT Selected, Stereo Anaglyph NOT Selected, Camera Separation 5% (deselected), Parallax Shift 0% (deselected); Background: Black. Structured source metadata values: 63.

VISIBLE OBSERVATION

A preserved presentation image is available for SIM². BENNETT records the visible source presentation without creating a new native measurement.

SOURCE-REPORTED RESULT

The source identifies this object as SIM², documents platform context as ZEISS Elyra, and records detected dye/channel descriptors as 405/DAPI; 488; 647.

LITERATURE CORRELATION

Consistent with peer-reviewed microscopy guidance that advanced-resolution outputs remain dependent on acquisition, reconstruction or localization quality control.

INTERPRETIVE LIMIT

Further reconstruction-dependent segmentation does not establish molecular dimensions, structure identity, or mechanism without independent support.

CLAIM CEILING

This tier supports a source-bounded statement that the historical SIM² evidence and documented settings are preserved for review; stronger biological or quantitative conclusions require compatible native data, controls and scientist review.

MODALITY ASSESSMENT / PART 8 OF 9

Single-molecule STORM / SOURCE EVIDENCE PRESERVED

DOCUMENTED SETTINGS

Platform: Bruker Vutara VXL. Objective: Olympus 60x/1.30 Silicon Oil objective. Platform: Bruker Vutara VXL Biplane Single Molecule Microscope, using an Olympus 60x/1.30 Silicon Oil objective, was used with the following parameters:. Detector/camera: Camera: Both Cameras. Timing: Exposure Time: 20 ms Selected; Super Resolution Camera Exposure Time: 20 ms; Widefield Camera Exposure Time: 100 ms. Illumination: Photoactivation/Imaging Laser: 0% Selected. Structured source metadata values: 80.

VISIBLE OBSERVATION

A preserved presentation image is available for Single-molecule STORM. BENNETT records the visible source presentation without creating a new native measurement.

SOURCE-REPORTED RESULT

The source identifies this object as Single-molecule STORM, documents platform context as Bruker Vutara VXL, and records detected dye/channel descriptors as 647.

LITERATURE CORRELATION

Consistent with peer-reviewed microscopy guidance that advanced-resolution outputs remain dependent on acquisition, reconstruction or localization quality control.

INTERPRETIVE LIMIT

Without localization tables, uncertainty, blinking, drift, and independent cluster evidence, the presentation cannot establish molecule count, cluster truth, exact precision, or molecular architecture.

CLAIM CEILING

This tier supports a source-bounded statement that the historical Single-molecule STORM evidence and documented settings are preserved for review; stronger biological or quantitative conclusions require compatible native data, controls and scientist review.

MODALITY ASSESSMENT / PART 9 OF 9

Control / SOURCE EVIDENCE PRESERVED

DOCUMENTED SETTINGS

Platform: Not stated in extracted source metadata. Objective: not explicitly stated. Acquisition: Z-Stack: 73 Slices (2.16 µm); Channels: 1; Scaling (Per Pixel): 0.059 µm X 0.059 µm X 0.030 µm; 0.059 µm X 0.059 µm; Image size (Pixels): 1341 X 1115; 1066 X 1066; Image Size (Pixels): 1341 X 1115; 1066 X 1066; Bit Depth: 16 Bit. Detector/camera: Imaging Device: GaAsP-Pmt3; Detector Type: GaAsP-PMT. Timing: Pixel Time: 0.26 µs; 0.32 µs; Frame Time: 5.63 s; 3.52 s. Illumination: Laser Wavelength: 639 nm @ 0.3%. Optical/scan: Pinhole: 1.00 AU / 65 µm; Scan Zoom: 1.5; 2.1; LSM Scan Speed: 11; Scan Direction: Bidirectional; Averaging: 8; Effective NA: 1.4. Processing: LSM Plus Mode: Filter: 8.1 (3D, Auto); Filter: 6.2 (3D, Auto). Structured source metadata values: 53.

VISIBLE OBSERVATION

A preserved presentation image is available for Control. BENNETT records the visible source presentation without creating a new native measurement.

SOURCE-REPORTED RESULT

The source identifies this object as Control, documents platform context as not stated, and records detected dye/channel descriptors as 405/DAPI; 488; 647.

LITERATURE CORRELATION

Consistent with peer-reviewed antibody-control guidance that a no-primary or related control bounds background but is not a complete specificity system.

INTERPRETIVE LIMIT

A control bounds the recorded comparison only; it does not establish universal specificity, zero background, zero cross-reactivity, or absence of free dye.

CLAIM CEILING

This tier supports a source-bounded statement that the historical Control evidence and documented settings are preserved for review; stronger biological or quantitative conclusions require compatible native data, controls and scientist review.

CROSS-MODALITY SYNTHESIS

The preserved PA-RR-000012 record contains the full ordered evidence sequence from Western blot through single-molecule STORM. Each modality retains its own acquisition and processing boundary.

Different acquisitions are not treated as a quantitative intensity ladder. Any continuity statement remains qualitative and source bounded.

BENNETT LITERATURE CORRELATION — SOURCES INDEPENDENTLY VERIFIED

BENNETT uses independently verified primary scientific sources to test whether the interpretation is scientifically consistent and properly bounded. Literature correlation does not retroactively validate the Identifyn dataset or replace scientist review.

- Antibody and microscopy evidence require orthogonal controls and modality-appropriate interpretation; presentation images alone do not establish analytical specificity.

- Advanced-resolution presentation depends on acquisition, reconstruction or localization quality control before numerical resolution, molecular dimensions or cluster identity can be claimed.

REFERENCES

1. Uhlen M, et al. A proposal for validation of antibodies. Nat Methods. 2016;13:823-827. doi:10.1038/nmeth.3995.
2. Gustafsson MGL. Surpassing the lateral resolution limit by a factor of two using structured illumination microscopy. J Microsc. 2000;198:82-87. doi:10.1046/j.1365-2818.2000.00710.x.
3. Sage D, et al. Quantitative evaluation of software packages for single-molecule localization microscopy. Nat Methods. 2015;12:717-724. doi:10.1038/nmeth.3442.

RELEASE BOUNDARY

This assessment remains a draft pending scientist review. No publication is authorized. Any future native-file analysis must enter BENNETT as a new evidence snapshot with routed engine authority, native-data QA, methods, limitations, and an independently reviewed claim ceiling.

SOURCE RECONCILIATION / QA / PROVENANCE

SOURCE STATUS - PRESERVED / AUTO-RECONCILED

Historical Identifyn source material was subjected to BENNETT retrospective QA. Original source state and correction history remain preserved in provenance.

HIGH CONFIDENCE - AUTO-RECONCILED

Airyscan / Scaling (Per Pixel): 35.29 nm X 35.29 nm X 30.00 nm -> 0.03529 µm X 0.03529 µm X 0.03000 µm. Both numerical magnitude and unit were normalized, then checked against the reported field dimensions; no unit label was changed alone. Supporting evidence: Image Size (Pixels)=945 X 703; Image Size (Scaled)=33.34 µm X 24.81 µm; PASS - INTERNALLY CONSISTENT. Documented sampling reproduces the reported physical field dimensions. Maximum field-dimension error 0.03%.

HIGH CONFIDENCE - AUTO-RECONCILED

SIM / Scaling (Per Pixel): 21.11 nm X 21.11 nm X 30.00 nm -> 0.02111 µm X 0.02111 µm X 0.03000 µm. Both numerical magnitude and unit were normalized, then checked against the reported field dimensions; no unit label was changed alone. Supporting evidence: Image Size (Pixels)=3155 X 2512; Image Size (Scaled)=66.61 µm X 53.03 µm; PASS - INTERNALLY CONSISTENT. Documented sampling reproduces the reported physical field dimensions. Maximum field-dimension error 0.01%.

HIGH CONFIDENCE - AUTO-RECONCILED

SIM² / Scaling (Per Pixel): 21.11 nm X 21.11 nm X 30.00 nm -> 0.02111 µm X 0.02111 µm X 0.03000 µm. Both numerical magnitude and unit were normalized, then checked against the reported field dimensions; no unit label was changed alone. Supporting evidence: Image Size (Pixels)=1557 X 1805; Image Size (Scaled)=32.87 µm X 38.11 µm; PASS - INTERNALLY CONSISTENT. Documented sampling reproduces the reported physical field dimensions. Maximum field-dimension error 0.02%.

HIGH CONFIDENCE - SOURCE-DERIVED METADATA CANONICALIZATION

Product identity / phosphosite: Blank structured canonical field -> Serine 1981. The phosphorylation site is explicitly stated in the preserved source product identity. Supporting evidence: Rabbit anti-Human ATM.p (Serine 1981) Recombinant Monoclonal

BENNETT

AI-POWERED BIOLOGICAL INTELLIGENCE

BENNETT EVIDENCE REVIEW COMPLETE

INTERPRETATION TO EVIDENCE

BENNETT has completed the bounded retrospective assessment.
The following pages switch ownership to the preserved Identifyn record.

IDENTiFYN®

IDENTIFYN PRESERVED SOURCE EVIDENCE

ORIGINAL RECORD BEGINS

Images, source methods, acquisition settings and provenance follow in the locked Stepdown order. Scientific wording is preserved; missing modalities are not invented.
A preserved control follows all available Stepdown tiers as supporting evidence.

PRODUCT-LEVEL STEPDOWN MAP

This dossier preserves the complete available evidence progression for PA-RR-000012. Each tier remains tied to its original image, source method, instrument context and cryptographic identity. A preserved control is retained as supporting evidence and appears after every resolution tier.

CANONICAL STEPDOWN TIER	EVIDENCE STAGE	INSTRUMENT	STATUS
1	Western blot	Azure Sapphire FL	PRESERVED
2	Widefield	ZEISS Axio Imager.M1	PRESERVED
3	Widefield SIM - Apotome	ZEISS Axio Observer.Z1/7 Apotome	PRESERVED
4	Confocal	ZEISS LSM 980	PRESERVED
5	Airyscan	ZEISS LSM 980	PRESERVED
6	SIM	ZEISS Elyra	PRESERVED
7	SIM²	ZEISS Elyra	PRESERVED
8	Single-molecule STORM	Bruker Vutara VXL	PRESERVED

INTERPRETIVE BOUNDARY

Ordering evidence by resolution tier does not make the modalities interchangeable. Each stage retains its acquisition environment and scientific limitations. This pilot organizes the record; it does not synthesize new biological claims.

ORIGINAL IMAGE EVIDENCE / WESTERN BLOT

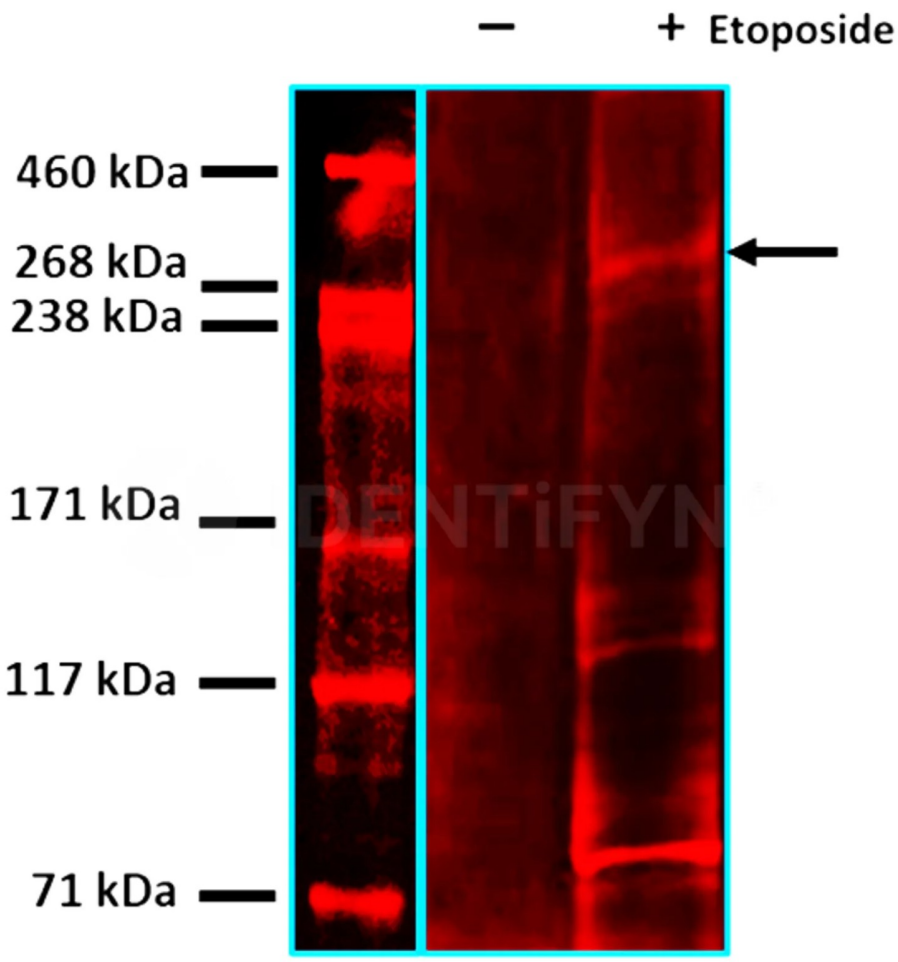

EVIDENCE TIER	Western blot
INSTRUMENT	Azure Sapphire FL
CELL MODEL	HeLa
DETECTED DYES	647
METADATA VALUES	11

STRUCTURED ACQUISITION METADATA / WESTERN BLOT

The values below were deterministically extracted from the preserved Identifyn method PDF text. They remain source-documented metadata, not new BENNETT measurements.

FIELD	SOURCE-DOCUMENTED VALUE
Platform / configuration	Azure Sapphire FL with Customizable Laser and Filter Modules, Enabling UV-NIR and Z-Plane Imaging.
Scanner	Azure Sapphire FL with Customizable Laser and Filter Modules, Enabling UV-NIR and Z-Plane Imaging.
Detection mode	Fluorescence
Laser	638 nm
Emission Filter	676 ± 37 nm
Detector	PMT
Intensity	L3
Pixel size	100 µm
Scan Speed	High
Quality	High
Focus	Membrane (0 µm in Z-axis)
Image	S. Khanal

SOURCE METHOD

The text below is carried from the preserved Identifyn source record. Typography and pagination have been normalized for this preservation dossier; scientific wording has not been editorially rewritten.

Identifyn Standards for Optical Microscopy Methods™

Identifyn® Primary Antibody

Rabbit anti-Human ATM.p (Serine 1981) Recombinant Monoclonal, IgG - (BLR031P)
Cat ID# PA-RR 000012

Expected MW: 350 kDa

HeLa cells were treated with 2 µM etoposide for 12 hours to induce DNA damage. Cells were homogenized using an ultrasonication probe and a nuclear lysis buffer, then centrifuged to pellet the cell debris. The lysate supernatant (100 µg) was mixed with NuPAGE™ LDS Sample Buffer (4X), heated at 80 °C for 10 min, and subjected to electrophoresis using NuPAGE™ Tris-Acetate Mini Protein Gels, 3 to 8%, 1.0 mm in a Mini Gel Tank. The Thermo Fisher's HiMark™ Pre-stained Protein Standard was used as a molecular weight marker.

Post electrophoresis, the proteins were transferred to a polyvinylidene difluoride (PVDF) membrane using the iBlot™ 3 Starter Kit PVDF. The transfer membrane was blocked with Blocker™ Casein for 1 hour, then washed 5 times with PBS. The blocked membrane was incubated with Rabbit anti-Human ATM.p (Serine 1981) Recombinant Monoclonal, IgG - (BLR031P) for 20 hours, followed by 5 washes with 1X PBS. Identifyn™ SRM Alexa Fluor™ 647 Affinity Purified Goat Anti-Rabbit IgG (H + L) was incubated for 1 hour and washed 5 times with 1X PBS. The membrane was dried for 10 minutes at room temperature before imaging.

Scanner = Azure Sapphire FL with Customizable Laser and Filter Modules, Enabling UV-NIR and Z-Plane Imaging.

Scan Settings

Detection mode = Fluorescence
Laser = 638 nm
Emission Filter = 676 ± 37 nm
Detector = PMT
Intensity = L3
Pixel size = 100 µm
Scan Speed = High
Quality = High
Focus = Membrane (0 µm in Z-axis)

Post Processing

NONE

Image: S. Khanal

SOURCE PROVENANCE

Catalog	PA-RR-000012
Stage	Western blot
Instrument	Azure Sapphire FL
Microscope configuration	Azure Sapphire FL with Customizable Laser and Filter Modules, Enabling UV-NIR and Z-Plane Imaging.
Structured source metadata values	11
Metadata source	PRESERVED_SOURCE_METHOD_PDF_TEXT
Cell model	HeLa
Image SHA-256	7FCE1170808A49B4491FC8F8479753E4C7B0C2EF5784E83D2D749B48A4C05C49
Method PDF SHA-256	F782F11CCD43E9A6A8AAAFC56762A4D7ACF54E97B04CA5CAE4B27288A346D407

ORIGINAL IMAGE EVIDENCE / WIDEFIELD

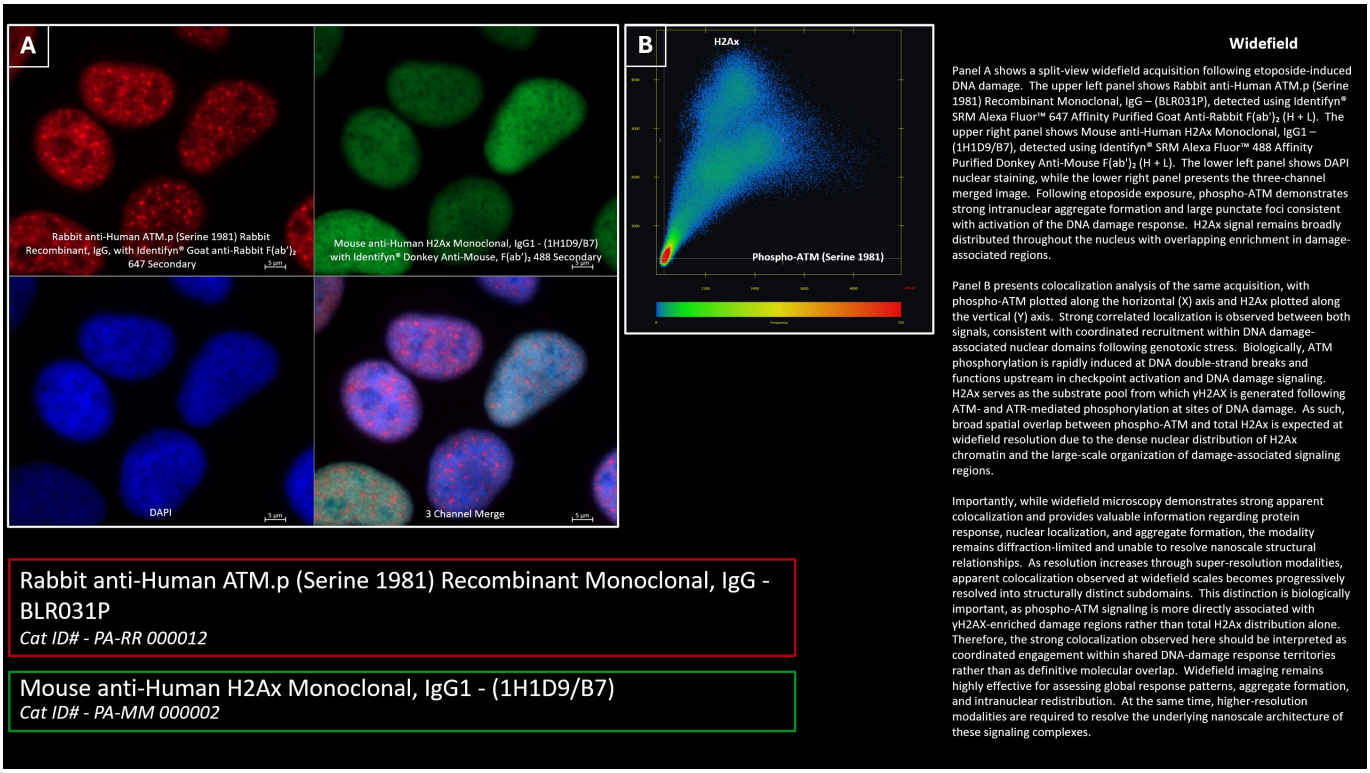

EVIDENCE TIER	Widefield
INSTRUMENT	ZEISS Axio Imager.M1
CELL MODEL	HeLa
DETECTED DYES	405/DAPI; 488; 647; 680
METADATA VALUES	38

STRUCTURED ACQUISITION METADATA / WIDEFIELD

The values below were deterministically extracted from the preserved Identifyn method PDF text. They remain source-documented metadata, not new BENNETT measurements.

FIELD	SOURCE-DOCUMENTED VALUE
Platform / configuration	Zeiss Axio Imager.M1 Widefield, using a Plan-Apochromat 63x/1.40 Oil M27, Axiocam 705, and X-Cite Xylis Lamp, was used with the following parameters for each dye:
Objective	Plan-Apochromat 63x/1.40 Oil M27
Channels	3
Scaling (Per Pixel)	0.110 µm X 0.110 µm
Image size (Pixels)	680 X 559
Image Size (Scaled)	74.48 µm X 61.22 µm
Bit Depth	14 Bit
Image Center Position	X: 0.00 mm, Y: 0.00 mm
ROI Center Offset	X: 0.00 µm, Y: 0.00 µm
Reflector	50 Cy 5 | 38 eGFP | 49 DAPI
Beam Splitter	660 | 495 | 395
Filter Excitation Wavelength	625 - 655 | 450 - 490 | 335 - 383
Filter Emission Wavelength	665 - 715 | 500 - 550 | 420 - 470
Contrast Method	Fluorescence
Light Source	X-Cite Xylis Lamp Intensity @ 15.00% | X-Cite Xylis Lamp Intensity @ 10.00%
Exposure Time	150 ms | 30 ms
Excitation Wavelength	653 | 493 | 353
Emission Wavelength	668 | 517 | 465
Effective NA	1.4
Imaging Device	Axiocam 705
Camera Adapter	1X
Depth of Focus	1.03 µm | 0.80 µm | 0.72 µm
Binning Mode	2,2
Image Measurement	Entire Field

SOURCE METHOD

The text below is carried from the preserved Identifyn source record. Typography and pagination have been normalized for this preservation dossier; scientific wording has not been editorially rewritten.

Identifyn Standards for Optical Microscopy Methods™

Identifyn® Primary Antibody

Rabbit anti-Human ATM.p (Serine 1981) Recombinant Monoclonal, IgG - (BLR031P)
Cat ID# PA-RR 000012

Mouse anti-Human H2Ax Monoclonal, IgG1 - (1H1D9/B7)
Cat ID# - PA-MM 000002

Identifyn® Secondary Antibodies

Identifyn® SRM Alexa Fluor™ 647 Affinity Purified Goat Anti-Rabbit, F(ab')□ (H + L)
Cat ID# - SA 000063

Identifyn® SRM Alexa Fluor™ 488 Affinity Purified Donkey Anti-Mouse, F(ab')□ (H + L)
Cat ID# - SA 000019

ATM (ataxia-telangiectasia mutated) is a crucial serine/threonine kinase that plays a central role in the DNA damage response (DDR), particularly in response to DNA double-strand breaks (DSBs). ATM's activation and subsequent phosphorylation cascades are essential for detecting DNA damage and initiating repair processes. Here's a detailed overview of how ATM is activated, its targets, and its role in the DDR:

Activation of ATM

In response to DNA damage, particularly DSBs, ATM is activated through a series of events:

Detection of DNA Breaks: ATM can sense DNA breaks by associating with the MRN complex (MRE11, RAD50, and NBS1). This complex recognizes DSBs, leading to ATM's recruitment to the damaged site.

Autophosphorylation: Upon detection of DNA damage, ATM autophosphorylates at serine 1981 (S1981), thereby activating it. This phosphorylation event is critical for ATM's kinase activity and its ability to phosphorylate downstream targets.

Dimer-to-Monomer Transition: In its inactive form, ATM is a dimer. It transitions to an active monomeric state upon activation, allowing it to interact with and phosphorylate various downstream proteins.

Phosphorylation Targets of ATM
Once activated, ATM phosphorylates many proteins involved in the DNA damage response, cell cycle regulation, and apoptosis. Here are some critical targets of ATM:

CHK2: ATM phosphorylates CHK2, a cell cycle checkpoint control kinase. This phosphorylation helps to halt the cell cycle, allowing time for DNA repair.

p53: ATM phosphorylates p53, activating this tumor suppressor, leading to cell cycle arrest or apoptosis if the damage is irreparable.

H2AX: ATM phosphorylates histone H2AX, forming γ-H2AX, a marker of DNA damage. This modification signals the presence of DSBs and recruits DNA repair machinery.

BRCA1: ATM's phosphorylation of BRCA1 is critical for homologous recombination, a key DNA repair pathway for DSBs.

NBS1: As part of the MRN complex, NBS1 phosphorylation by ATM enhances the complex's DNA repair functions.

53BP1: ATM phosphorylation of 53BP1 helps recruit this protein to sites of DSBs, thereby guiding repair pathways such as non-homologous end joining (NHEJ).

Role of ATM Phosphorylation in DNA Repair

ATM-mediated phosphorylation plays a central role in coordinating the DNA damage response:
Signal Propagation: Phosphorylation cascades initiated by ATM amplify the signal in response to DNA damage, ensuring an efficient response.

Recruitment of Repair Machinery: Phosphorylation of specific proteins helps recruit DNA repair complexes to the sites of DNA damage.

Cell Cycle Regulation: ATM activation can lead to cell cycle checkpoints, preventing cells with damaged DNA from dividing.

Apoptosis: If the DNA damage is too severe to repair, ATM's activation can lead to apoptosis, preventing the propagation of damaged cells

ATM's phosphorylation in response to DNA damage is crucial for detecting DNA double-strand breaks and coordinating the DNA damage response. By phosphorylating a range of critical proteins, ATM orchestrates a complex signaling network that facilitates DNA repair, cell cycle regulation, and apoptosis, thereby maintaining genomic stability.

Method

HeLa cells were grown on acid-etched #1.5H cover glass to ~50% confluency, DNA damage was induced by treatment with 2 µM Etoposide-spiked complete growth media for 12 hours, followed by -20 °C methanol fixation and blocking with Thermo Fisher Fish Serum Blocker (cat#37527X3). The primary antibody, Rabbit anti-Human ATM.p (Serine 1981) Recombinant Monoclonal, IgG - (BLR031P), was incubated at room temperature for 1 hour at a 1:250 dilution. Cells were washed 3X in PBS. Identifyn® SRM Alexa Fluor™ 647 Affinity Purified Goat Anti-Rabbit, F(ab')□ (H + L) was incubated at room temperature for 1 hour at a dilution of 1:1000. Cells were washed 5X in PBS.

The second primary antibody, Mouse anti-Human H2Ax Monoclonal, IgG1 - (1H1D9/B7), was then incubated for 1 hour at room temperature at a dilution of 1:250. Cells were washed 3X in PBS.
Identifyn® SRM Alexa Fluor™ 488 Affinity Purified Donkey Anti-Mouse, F(ab')□ (H + L) was incubated for 1 hour at room temperature at a dilution of 1:1000. Cells were washed 5X in PBS and mounted using ProLong™ Diamond Antifade Mountant with DAPI cat#P36962.

Microscope

Zeiss Axio Imager.M1 Widefield, using a Plan-Apochromat 63x/1.40 Oil M27, Axiocam 705, and X-Cite Xylis Lamp, was used with the following parameters for each dye:

Single Plane (2D)

Channels = 3
Scaling (Per Pixel) = 0.110 µm X 0.110 µm
Image size (Pixels) = 680 X 559
Image Size (Scaled) = 74.48 µm X 61.22 µm
Bit Depth = 14 Bit
Image Center Position = X: 0.00 mm, Y: 0.00 mm
ROI Center Offset = X: 0.00 µm, Y: 0.00 µm

647 -

Reflector = 50 Cy 5
Beam Splitter = 660
Filter Excitation Wavelength = 625 - 655
Filter Emission Wavelength = 665 - 715
Contrast Method = Fluorescence
Light Source = X-Cite Xylis Lamp Intensity @ 15.00%
Exposure Time = 150 ms
Excitation Wavelength = 653
Emission Wavelength = 668
Effective NA = 1.4
Imaging Device = Axiocam 705
Camera Adapter = 1X
Depth of Focus = 1.03 µm
Binning Mode = 2,2

488 -

Reflector = 38 eGFP
Beam Splitter = 495
Filter Excitation Wavelength = 450 - 490
Filter Emission Wavelength = 500 - 550
Contrast Method = Fluorescence
Light Source = X-Cite Xylis Lamp Intensity @ 15.00%
Exposure Time = 150 ms
Excitation Wavelength = 493
Emission Wavelength = 517
Effective NA = 1.4
Imaging Device = Axiocam 705
Camera Adapter = 1X
Depth of Focus = 0.80 µm
Binning Mode = 2,2

DAPI -

Reflector = 49 DAPI
Beam Splitter = 395
Filter Excitation Wavelength = 335 - 383
Filter Emission Wavelength = 420 - 470
Contrast Method = Fluorescence
Light Source = X-Cite Xylis Lamp Intensity @ 10.00%
Exposure Time = 30 ms
Excitation Wavelength = 353
Emission Wavelength = 465
Effective NA = 1.4
Imaging Device = Axiocam 705
Camera Adapter = 1X
Depth of Focus = 0.72 µm
Binning Mode = 2,2

Split View - Panel A

The top-left panel shows Rabbit anti-Human ATM.p (Serine 1981) Recombinant Monoclonal, IgG - (BLR031P), visualized using Identifyn® SRM Alexa Fluor™ 647 affinity-purified Goat Anti-Rabbit F(ab')□ (H + L). The top-right panel shows Mouse anti-Human H2Ax Monoclonal, IgG1 - (1H1D9/B7), visualized using Identifyn® SRM Alexa Fluor™ 488 affinity-purified Donkey Anti-Mouse F(ab')□ (H + L). The lower-left panel shows DAPI nuclear staining, and the bottom-right panel shows the three-channel merged image.

Colocalization View - Panel B

Horizontal Axis - AF647, Threshold 190, Range Auto - Phospho-ATM
Vertical Axis - AF488, Threshold 332, Range Auto - H2Ax
Image Measurement = Entire Field

Colocalization analysis of Phospho-ATM (X-axis) and H2AX (Y-axis) was performed across the entire image acquisition.

Summary

Panel A shows a split-view widefield acquisition following etoposide-induced DNA damage. The upper left panel shows Rabbit anti-Human ATM.p (Serine 1981) Recombinant Monoclonal, IgG - (BLR031P), detected using Identifyn® SRM Alexa Fluor™ 647 Affinity Purified Goat Anti-Rabbit F(ab')□ (H + L). The upper right panel shows Mouse anti-Human H2Ax Monoclonal, IgG1 - (1H1D9/B7), detected using Identifyn® SRM Alexa Fluor™ 488 Affinity Purified Donkey Anti-Mouse F(ab')□ (H + L). The lower-left panel shows DAPI nuclear staining, while the lower-right panel shows the three-channel merged image. Following etoposide exposure, phospho-ATM demonstrates strong intranuclear aggregate formation and large punctate foci consistent with activation of the DNA damage response. H2Ax signal remains broadly distributed throughout the nucleus with overlapping enrichment in damage-associated regions.

Panel B presents colocalization analysis of the same acquisition, with phospho-ATM plotted along the horizontal (X) axis and H2Ax plotted along the vertical (Y) axis. Strong correlated localization is observed between both signals, consistent with coordinated recruitment within DNA damage-associated nuclear domains following genotoxic stress. Biologically, ATM phosphorylation is rapidly induced at DNA double-strand breaks and functions upstream in checkpoint activation and DNA damage signaling. H2Ax serves as the substrate pool from which γH2AX is generated following ATM- and ATR-mediated phosphorylation at sites of DNA damage. As such, broad spatial overlap between phospho-ATM and total H2Ax is expected at widefield resolution due to the dense nuclear distribution of H2Ax chromatin and the large-scale organization of damage-associated signaling regions.

Importantly, while widefield microscopy demonstrates strong apparent colocalization and provides valuable information regarding protein response, nuclear localization, and aggregate formation, the modality remains diffraction-limited and unable to resolve nanoscale structural relationships. As resolution increases through super-resolution modalities, apparent colocalization observed at widefield scales becomes progressively resolved into structurally distinct subdomains. This distinction is biologically important, as phospho-ATM signaling is more directly associated with γH2AX-enriched damage regions rather than total H2Ax distribution alone. Therefore, the strong colocalization observed here should be interpreted as coordinated engagement within shared DNA-damage response territories rather than as definitive molecular overlap. Widefield imaging remains highly effective for assessing global response patterns, aggregate formation, and intranuclear redistribution. At the same time, higher-resolution modalities are required to resolve the underlying nanoscale architecture of these signaling complexes.

Image Correction

NONE

Image by E.F.Simon
Image Analysis and Data Presentation by B.T. Bennett

SOURCE PROVENANCE

Catalog	PA-RR-000012
Stage	Widefield
Instrument	ZEISS Axio Imager.M1
Microscope configuration	Zeiss Axio Imager.M1 Widefield, using a Plan-Apochromat 63x/1.40 Oil M27, Axiocam 705, and X-Cite Xylis Lamp, was used with the following parameters for each dye:
Structured source metadata values	38
Metadata source	PRESERVED_SOURCE_METHOD_PDF_TEXT
Cell model	HeLa
Image SHA-256	65821CA6B5C1DEFF66140EC05DF6AB515895E51B3397D7C6DBC91B19CBD62A57
Method PDF SHA-256	7A9A038D384B433FFB531F1D1D10D11130E349C7547AA7D8A3B8B8E4C47E745F

ORIGINAL IMAGE EVIDENCE / WIDEFIELD SIM - APOTOME

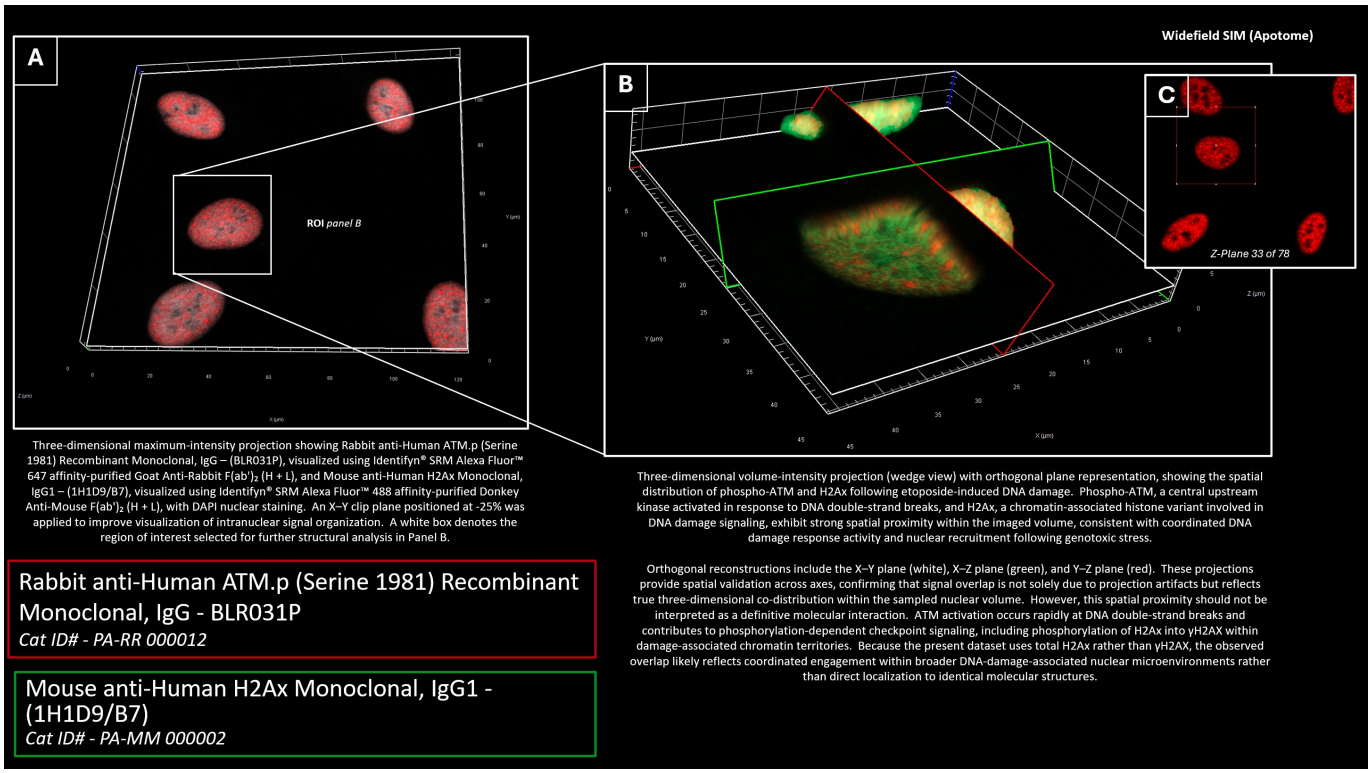

Three-dimensional maximum-intensity projection showing Rabbit anti-Human ATM.p (Serine 1981) Recombinant Monoclonal, IgG – (BLR031P), visualized using Identifyn® SRM Alexa Fluor™ 647 affinity-purified Goat Anti-Rabbit F(ab')$_2$ (H + L), and Mouse anti-Human H2Ax Monoclonal, IgG1 – (1H1D9/B7), visualized using Identifyn® SRM Alexa Fluor™ 488 affinity-purified Donkey Anti-Mouse F(ab')$_2$ (H + L), with DAPI nuclear staining. An X–Y clip plane positioned at -25% was applied to improve visualization of intranuclear signal organization. A white box denotes the region of interest selected for further structural analysis in Panel B.

Three-dimensional volume-intensity projection (wedge view) with orthogonal plane representation, showing the spatial distribution of phospho-ATM and H2Ax following etoposide-induced DNA damage. Phospho-ATM, a central upstream kinase activated in response to DNA double-strand breaks, and H2Ax, a chromatin-associated histone variant involved in DNA damage signaling, exhibit strong spatial proximity within the imaged volume, consistent with coordinated DNA damage response activity and nuclear recruitment following genotoxic stress.

Orthogonal reconstructions include the X–Y plane (white), X–Z plane (green), and Y–Z plane (red). These projections provide spatial validation across axes, confirming that signal overlap is not solely due to projection artifacts but reflects true three-dimensional co-distribution within the sampled nuclear volume. However, this spatial proximity should not be interpreted as a definitive molecular interaction. ATM activation occurs rapidly at DNA double-strand breaks and contributes to phosphorylation-dependent checkpoint signaling, including phosphorylation of H2Ax into γH2AX within damage-associated chromatin territories. Because the present dataset uses total H2Ax rather than γH2AX, the observed overlap likely reflects coordinated engagement within broader DNA-damage-associated nuclear microenvironments rather than direct localization to identical molecular structures.

Rabbit anti-Human ATM.p (Serine 1981) Recombinant Monoclonal, IgG - BLR031P
Cat ID# - PA-RR 000012

Mouse anti-Human H2Ax Monoclonal, IgG1 - (1H1D9/B7)
Cat ID# - PA-MM 000002

EVIDENCE TIER	Widefield SIM - Apotome
INSTRUMENT	ZEISS Axio Observer.Z1/7 Apotome
CELL MODEL	HeLa
DETECTED DYES	405/DAPI; 488; 647
METADATA VALUES	50

STRUCTURED ACQUISITION METADATA / WIDEFIELD SIM - APOTOME

The values below were deterministically extracted from the preserved Identifyn method PDF text. They remain source-documented metadata, not new BENNETT measurements.

FIELD	SOURCE-DOCUMENTED VALUE
Platform / configuration	Zeiss Axio Observer.Z1/7 Apotome SIM, using an EC Plan-Neofluar 63x/1.25 Oil M27, Axiocam 807 Mono, and X-Cite Xylis Lamp was used with the following parameters for each dye:
Objective	EC Plan-Neofluar 63x/1.25 Oil M27
Z-Stack	78 Slices (7.7 µm)
Channels	2
Scaling (Per Pixel)	0.143 µm X 0.143 µm X 0.100 µm
Image Size (Pixels)	864 X 791 | 324 X 317
Image Size (Scaled)	123.43 µm X 113.00 µm | 46.29 µm X 45.29 µm
Bit Depth	14 Bit
Image Center Position	X: 50.87 mm, Y: 48.68 mm
Stage Position	X: 50.87 mm, Y: 48.68 mm
ROI Center Offset	X: 1.14 µm, Y: 0.00 µm
Reflector	50 Cy 5 | 38 HE eGFP
Beam Splitter	660 | 495
Filter Excitation Wavelength	625 - 655 | 450 - 490
Filter Emission Wavelength	665 - 715 | 500 - 550
Contrast Method	Fluorescence
Light Source	X-Cite Xylis Lamp Intensity @ 10.00% | X-Cite Xylis Lamp Intensity @ 25.00%
Exposure Time	100 ms | 250 ms
Excitation Wavelength	653 | 493
Emission Wavelength	668 | 517
Effective NA	1.25
Imaging Device	Axiocam 807 Mono
Camera Adapter	1X
Depth of Focus	1.30 µm | 1.00 µm
Binning Mode	2,2
Apotome SIM Image Processing	Display Mode "Optical Sectioning" - enabled correction selected.
3D Maximum Projection	Precise
Appearance	Threshold 13% all channels, Ramp 0% all channels, Maximum 100% all channels
Background	Black
Light	Brightness 100%, Enabled Tone Mapping
Projection	View Angle 35°, Scale Z 100%, Reverse Z-Axis NOT Selected, Stereo Anaglyph NOT Selected, Camera Separation 5% (deselected), Parallax Shift 0% (deselected)
X-Y	Activate was selected, textured opaque was chosen, and a white outline of the clipped perimeter was shown; Clip Back was selected, and Clip Front was NOT selected.

FIELD	SOURCE-DOCUMENTED VALUE
Position of Clip	-25% | -44% | 0%
Clip X	0°
Clip Z	0°
X-Z	Activate was selected, textured opaque was chosen, and a green outline of the clipped perimeter was shown; Clip Back was selected, and Clip Front was NOT selected.
Clip Y	30° | -30°
Y-Z	Activate was selected, textured opaque was chosen, and a red outline of the clipped perimeter was shown; Clip Back was selected, and Clip Front was NOT selected.

SOURCE METHOD

The text below is carried from the preserved Identifyn source record. Typography and pagination have been normalized for this preservation dossier; scientific wording has not been editorially rewritten.

Identifyn Standards for Optical Microscopy Methods™

Identifyn® Primary Antibody

Rabbit anti-Human ATM.p (Serine 1981) Recombinant Monoclonal, IgG - (BLR031P)
Cat ID# PA-RR 000012

Mouse anti-Human H2Ax Monoclonal, IgG1 - (1H1D9/B7)
Cat ID# - PA-MM 000002

Identifyn® Secondary Antibodies

Identifyn® SRM Alexa Fluor™ 647 Affinity Purified Goat Anti-Rabbit, F(ab')□ (H + L)
Cat ID# - SA 000063

Identifyn® SRM Alexa Fluor™ 488 Affinity Purified Donkey Anti-Mouse, F(ab')□ (H + L)
Cat ID# - SA 000019

ATM (ataxia-telangiectasia mutated) is a crucial serine/threonine kinase that plays a central role in the DNA damage response (DDR), particularly in response to DNA double-strand breaks (DSBs). ATM's activation and subsequent phosphorylation cascades are essential for detecting DNA damage and initiating repair processes. Here's a detailed overview of how ATM is activated, its targets, and its role in the DDR:

Activation of ATM

In response to DNA damage, particularly DSBs, ATM is activated through a series of events:

Detection of DNA Breaks: ATM can sense DNA breaks by associating with the MRN complex (MRE11, RAD50, and NBS1). This complex recognizes DSBs, leading to ATM's recruitment to the damaged site.

Autophosphorylation: Upon detection of DNA damage, ATM autophosphorylates at serine 1981 (S1981), thereby activating it. This phosphorylation event is critical for ATM's kinase activity and its ability to phosphorylate downstream targets.

Dimer-to-Monomer Transition: In its inactive form, ATM is a dimer. It transitions to an active monomeric state upon activation, allowing it to interact with and phosphorylate various downstream proteins.

Phosphorylation Targets of ATM
Once activated, ATM phosphorylates many proteins involved in the DNA damage response, cell cycle regulation, and apoptosis. Here are some critical targets of ATM:

CHK2: ATM phosphorylates CHK2, a cell cycle checkpoint control kinase. This phosphorylation helps to halt the cell cycle, allowing time for DNA repair.

p53: ATM phosphorylates p53, activating this tumor suppressor, leading to cell cycle arrest or apoptosis if the damage is irreparable.

H2AX: ATM phosphorylates histone H2AX, forming γ-H2AX, a marker of DNA damage. This modification helps signal the presence of DSBs and recruit DNA repair machinery.

BRCA1: ATM's phosphorylation of BRCA1 is critical for homologous recombination, a key DNA repair pathway for DSBs.

NBS1: As part of the MRN complex, NBS1 phosphorylation by ATM enhances the complex's DNA repair functions.

53BP1: ATM phosphorylation of 53BP1 helps recruit this protein to sites of DSBs, thereby guiding repair pathways such as non-homologous end joining (NHEJ).

Role of ATM Phosphorylation in DNA Repair

ATM-mediated phosphorylation plays a central role in coordinating the DNA damage response:
Signal Propagation: Phosphorylation cascades initiated by ATM amplify the signal in response to DNA damage, ensuring an efficient response.

Recruitment of Repair Machinery: Phosphorylation of specific proteins helps recruit DNA repair complexes to the sites of DNA damage.

Cell Cycle Regulation: ATM activation can lead to cell cycle checkpoints, preventing cells with damaged DNA from dividing.

Apoptosis: If the DNA damage is too severe to repair, ATM's activation can lead to apoptosis, preventing the propagation of damaged cells

ATM's phosphorylation in response to DNA damage is crucial for detecting DNA double-strand breaks and coordinating the DNA damage response. By phosphorylating a range of critical proteins, ATM orchestrates a complex signaling network that facilitates DNA repair, cell cycle regulation, and apoptosis, thereby maintaining genomic stability.

Method

HeLa cells were grown on acid-etched #1.5H cover glass to ~50% confluency, DNA damage was induced by treatment with 2 µM Etoposide-spiked complete growth media for 12 hours, followed by -20 °C methanol fixation and blocking with Thermo Fisher Fish Serum Blocker (cat#37527X3). The primary antibody, Rabbit anti-Human ATM.p (Serine 1981) Recombinant Monoclonal, IgG - (BLR031P), was incubated at room temperature for 1 hour at a 1:250 dilution. Cells were washed 3X in PBS. Identifyn® SRM Alexa Fluor™ 647 Affinity Purified Goat Anti-Rabbit, F(ab')□ (H + L) was incubated at room temperature for 1 hour at a dilution of 1:1000. Cells were washed 5X in PBS.

The second primary antibody, Mouse anti-Human H2Ax Monoclonal, IgG1 - (1H1D9/B7), was then incubated for 1 hour at room temperature at a dilution of 1:250. Cells were washed 3X in PBS.
Identifyn® SRM Alexa Fluor™ 488 Affinity Purified Donkey Anti-Mouse, F(ab')□ (H + L) was incubated for 1 hour at room temperature at a dilution of 1:1000. Cells were washed 5X in PBS and mounted using ProLong™ Diamond Antifade Mountant with DAPI cat#P36962.

Microscope

Zeiss Axio Observer.Z1/7 Apotome SIM, using an EC Plan-Neofluar 63x/1.25 Oil M27, Axiocam 807 Mono, and X-Cite Xylis Lamp was used with the following parameters for each dye:

Z Stack - (3D) - Panel A, 3-Dimensional Maximum Projection, and Panel C, Z-Plane 33 of 78

Z-Stack = 78 Slices (7.7 µm)

Channels = 2
Scaling (Per Pixel) = 0.143 µm X 0.143 µm X 0.100 µm
Image Size (Pixels) = 864 X 791
Image Size (Scaled) = 123.43 µm X 113.00 µm
Bit Depth = 14 Bit
Image Center Position = X: 50.87 mm, Y: 48.68 mm
Stage Position = X: 50.87 mm, Y: 48.68 mm
ROI Center Offset = X: 1.14 µm, Y: 0.00 µm

Z Stack - (3D) - Panel B, ROI, 3-Dimensional orthogonal Cut Plane

Z-Stack = 78 Slices (7.7 µm)

Channels = 2
Scaling (Per Pixel) = 0.143 µm X 0.143 µm X 0.100 µm
Image Size (Pixels) = 324 X 317
Image Size (Scaled) = 46.29 µm X 45.29 µm
Bit Depth = 14 Bit
Image Center Position = X: 50.87 mm, Y: 48.68 mm
Stage Position = X: 50.87 mm, Y: 48.68 mm
ROI Center Offset = X: 1.14 µm, Y: 0.00 µm

647 -

Reflector = 50 Cy 5
Beam Splitter = 660
Filter Excitation Wavelength = 625 - 655
Filter Emission Wavelength = 665 - 715
Contrast Method = Fluorescence
Light Source = X-Cite Xylis Lamp Intensity @ 10.00%
Exposure Time = 100 ms
Excitation Wavelength = 653
Emission Wavelength = 668
Effective NA = 1.25
Imaging Device = Axiocam 807 Mono
Camera Adapter = 1X
Depth of Focus = 1.30 µm
Binning Mode = 2,2

488 -

Reflector = 38 HE eGFP
Beam Splitter = 495
Filter Excitation Wavelength = 450 - 490
Filter Emission Wavelength = 500 - 550
Contrast Method = Fluorescence
Light Source = X-Cite Xylis Lamp Intensity @ 25.00%
Exposure Time = 250 ms
Excitation Wavelength = 493
Emission Wavelength = 517
Effective NA = 1.25
Imaging Device = Axiocam 807 Mono
Camera Adapter = 1X
Depth of Focus = 1.00 µm
Binning Mode = 2,2

Post Processing - SIM Processing

Apotome SIM Image Processing = Display Mode "Optical Sectioning" - enabled correction selected. Normalization, Phase Corrector, Fourier Filter, and Deconvolution were NOT used. 3D Image Processing

3D Image Processing - Panel A

3D Maximum Projection = Precise
Appearance = Threshold 13% all channels, Ramp 0% all channels, Maximum 100% all channels
Background = Black
Light = Brightness 100%, Enabled Tone Mapping
Projection = View Angle 35°, Scale Z 100%, Reverse Z-Axis NOT Selected, Stereo Anaglyph NOT Selected, Camera Separation 5% (deselected), Parallax Shift 0% (deselected)

Clipping Image Process - Panel A

An X-Y clip plane is introduced in Panel A to highlight the phospho-ATM and the H2Ax within the nuclear compartment.

X-Y = Activate was selected, textured opaque was chosen, and a white outline of the clipped perimeter was shown; Clip Back was selected, and Clip Front was NOT selected.

Position of Clip = -25%
Clip X = 0°
Clip Z = 0°

3D Image Processing - Panel B

3D Maximum Projection = Precise
Appearance = Threshold 13% all channels, Ramp 0% all channels, Maximum 100% all channels
Background = Black
Light = Brightness 100%, Enabled Tone Mapping
Projection = View Angle 35°, Scale Z 100%, Reverse Z-Axis NOT Selected, Stereo Anaglyph NOT Selected, Camera Separation 5% (deselected), Parallax Shift 0% (deselected)

Clipping Image Process - Panel B

Clipping planes are introduced in Panel B to highlight the phospho-ATM and the H2Ax within the nuclear compartment by adjusting or cutting away portions of the image using a triple-wedge cut, removing parts of the image in the X-Y, X-Z, and Y-Z planes.

X-Y = Activate was selected, textured opaque was chosen, and a white outline of the clipped perimeter was shown; Clip Back was selected, and Clip Front was NOT selected.

Position of Clip = -44%
Clip X = 0°
Clip Z = 0°

X-Z = Activate was selected, textured opaque was chosen, and a green outline of the clipped perimeter was shown; Clip Back was selected, and Clip Front was NOT selected.

Position of Clip = 0%
Clip Y = 30°
Clip Z = 0°

Y-Z = Activate was selected, textured opaque was chosen, and a red outline of the clipped perimeter was shown; Clip Back was selected, and Clip Front was NOT selected.

Position of Clip = 0%
Clip Y = -30°
Clip Z = 0°

Single Plane (2D) - Panel C

Shows a two-dimensional view of the original image acquisition at Z-plane 33 of 78 for the phospho-ATM 647 channel alone. The region of interest (ROI) corresponding to the structural analysis shown in Panel B is indicated, providing an isolated view of phospho-ATM aggregate formation and intranuclear organization following etoposide-induced DNA damage.

Summary

Panel A demonstrates a three-dimensional maximum-intensity projection of phospho-ATM and H2Ax following etoposide-induced DNA damage. Rabbit anti-Human ATM.p (Serine 1981) Recombinant Monoclonal, IgG - (BLR031P), visualized using Identifyn® SRM Alexa Fluor™ 647 affinity-purified Goat Anti-Rabbit F(ab')□ (H + L), demonstrates prominent intranuclear aggregate formation and focal redistribution consistent with activation of the ATM-mediated DNA damage response pathway. Mouse anti-Human H2Ax Monoclonal, IgG1 - (1H1D9/B7), visualized using Identifyn® SRM Alexa Fluor™ 488 affinity-purified Donkey Anti-Mouse F(ab')□ (H + L), remains broadly distributed throughout the chromatin compartment, reflecting the constitutive nuclear localization of H2Ax as a histone substrate involved in DNA damage signaling. An X-Y clip plane positioned at -25% improves visualization of the internal nuclear organization, while the boxed region identifies the area selected for further volumetric analysis in Panel B.

Panel B presents a three-dimensional wedge-view orthogonal reconstruction of the selected region of interest. Orthogonal projections across the X-Y, X-Z, and Y-Z planes demonstrate strong spatial proximity between phospho-ATM and H2Ax within DNA damage-associated nuclear territories. Biologically, ATM phosphorylation is rapidly induced following DNA double-strand break formation and functions as a central upstream regulator of checkpoint activation, chromatin signaling, and DNA repair coordination. ATM-mediated phosphorylation of H2Ax into γH2AX represents one of the earliest amplification events in DNA damage signaling; however, because the present

dataset measures total H2Ax rather than γH2AX specifically, the observed overlap likely reflects broader chromatin-associated recruitment and DNA damage-associated nuclear organization rather than direct molecular colocalization. The orthogonal projections confirm that the observed signal overlap is present throughout the three-dimensional nuclear volume and not solely due to the planar projection artifact.

Panel C provides a two-dimensional view of the original acquisition at Z-plane 33 of 78 for the phospho-ATM 647 channel alone, with the region of interest corresponding to Panel B identified. This isolated phospho-ATM view demonstrates extensive aggregate and punctate signal formation following etoposide treatment, consistent with localized activation and concentration of ATM signaling domains at sites of DNA damage response activity.

Collectively, the dataset demonstrates robust nuclear recruitment and redistribution of phospho-ATM following genotoxic stress, accompanied by strong apparent overlap with H2Ax-containing chromatin territories. At diffraction-limited and near-diffraction-limited resolution, these modalities are highly effective for assessing global response patterns, aggregate formation, and spatial nuclear organization. However, because total H2Ax is broadly distributed throughout chromatin and because widefield and volumetric reconstructions remain structurally conflated at the nanoscale, the observed overlap should be interpreted as coordinated engagement within shared DNA damage response microenvironments rather than definitive molecular interaction. Higher-resolution super-resolution approaches remain necessary to resolve the underlying nanoscale architecture and true structural relationships between ATM signaling complexes and phosphorylated chromatin domains.

Image Correction

NONE

Image by E.F.Simon
Image Analysis and Data Presentation by B.T. Bennett

SOURCE PROVENANCE

Catalog	PA-RR-000012
Stage	Widefield SIM - Apotome
Instrument	ZEISS Axio Observer.Z1/7 Apotome
Microscope configuration	Zeiss Axio Observer.Z1/7 Apotome SIM, using an EC Plan-Neofluar 63x/1.25 Oil M27, Axiocam 807 Mono, and X-Cite Xylis Lamp was used with the following parameters for each dye:
Structured source metadata values	50
Metadata source	PRESERVED_SOURCE_METHOD_PDF_TEXT
Cell model	HeLa
Image SHA-256	A8F6617AF7CB4CC66A050B2CB395ED2DB928555B2422E485F9D4A59744C87512
Method PDF SHA-256	24603A0FD5AE7F2243C577425F29016F94E71AE81D39FCA731301B5B286FA250

ORIGINAL IMAGE EVIDENCE / CONFOCAL

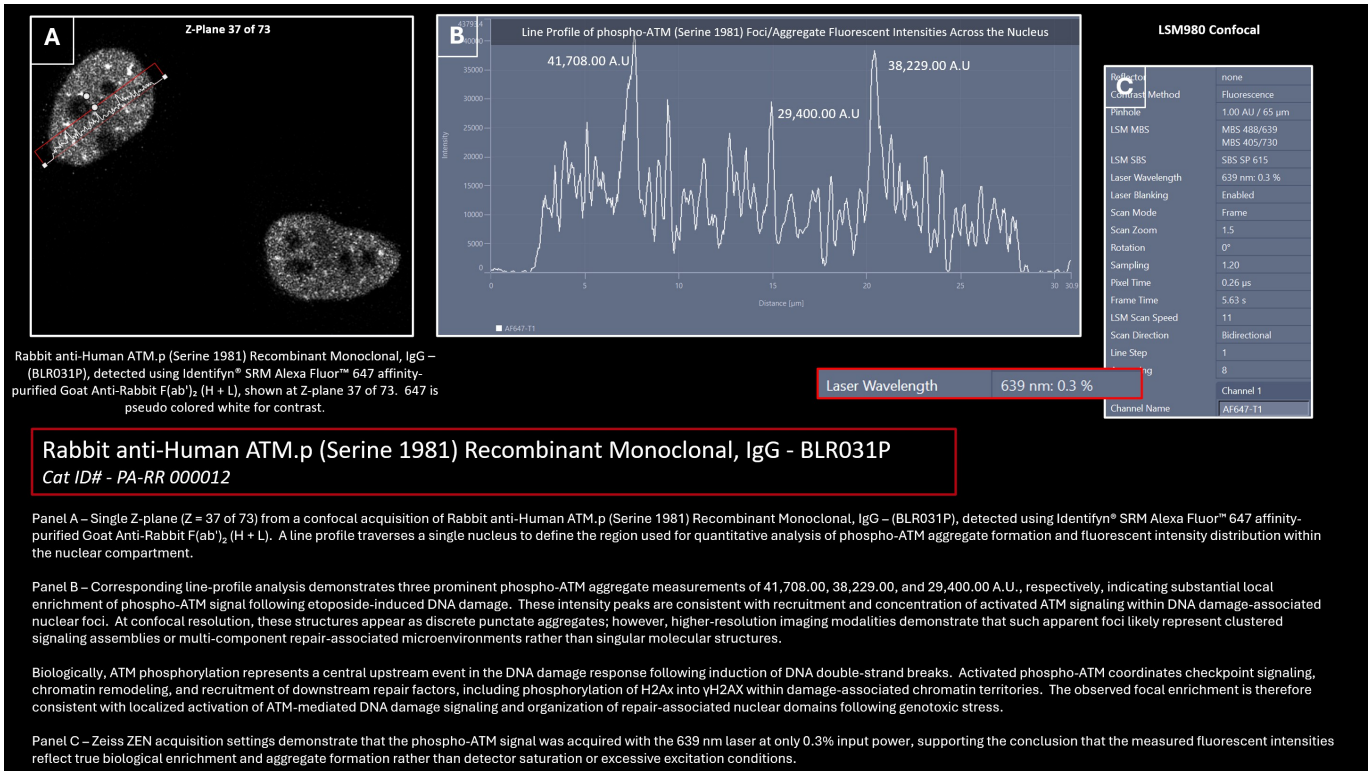

Rabbit anti-Human ATM.p (Serine 1981) Recombinant Monoclonal, IgG – (BLR031P), detected using Identifyn® SRM Alexa Fluor™ 647 affinity-purified Goat Anti-Rabbit F(ab')$_2$ (H + L), shown at Z-plane 37 of 73. 647 is pseudo colored white for contrast.

Rabbit anti-Human ATM.p (Serine 1981) Recombinant Monoclonal, IgG - BLR031P
Cat ID# - PA-RR 000012

Panel A – Single Z-plane (Z = 37 of 73) from a confocal acquisition of Rabbit anti-Human ATM.p (Serine 1981) Recombinant Monoclonal, IgG – (BLR031P), detected using Identifyn® SRM Alexa Fluor™ 647 affinity-purified Goat Anti-Rabbit F(ab')$_2$ (H + L). A line profile traverses a single nucleus to define the region used for quantitative analysis of phospho-ATM aggregate formation and fluorescent intensity distribution within the nuclear compartment.

Panel B – Corresponding line-profile analysis demonstrates three prominent phospho-ATM aggregate measurements of 41,708.00, 38,229.00, and 29,400.00 A.U., respectively, indicating substantial local enrichment of phospho-ATM signal following etoposide-induced DNA damage. These intensity peaks are consistent with recruitment and concentration of activated ATM signaling within DNA damage-associated nuclear foci. At confocal resolution, these structures appear as discrete punctate aggregates; however, higher-resolution imaging modalities demonstrate that such apparent foci likely represent clustered signaling assemblies or multi-component repair-associated microenvironments rather than singular molecular structures.

Biologically, ATM phosphorylation represents a central upstream event in the DNA damage response following induction of DNA double-strand breaks. Activated phospho-ATM coordinates checkpoint signaling, chromatin remodeling, and recruitment of downstream repair factors, including phosphorylation of H2Ax into γH2AX within damage-associated chromatin territories. The observed focal enrichment is therefore consistent with localized activation of ATM-mediated DNA damage signaling and organization of repair-associated nuclear domains following genotoxic stress.

Panel C – Zeiss ZEN acquisition settings demonstrate that the phospho-ATM signal was acquired with the 639 nm laser at only 0.3% input power, supporting the conclusion that the measured fluorescent intensities reflect true biological enrichment and aggregate formation rather than detector saturation or excessive excitation conditions.

EVIDENCE TIER	Confocal
INSTRUMENT	ZEISS LSM 980
CELL MODEL	HeLa
DETECTED DYES	405/DAPI; 488; 647
METADATA VALUES	46

STRUCTURED ACQUISITION METADATA / CONFOCAL

The values below were deterministically extracted from the preserved Identifyn method PDF text. They remain source-documented metadata, not new BENNETT measurements.

FIELD	SOURCE-DOCUMENTED VALUE
Platform / configuration	Zeiss LSM980 Confocal with NIR Detection, Axio Observer.Z1/7, using a Plan-Apochromat 63x/1.40 Oil DIC M27, was used with the following parameters for each dye:
Objective	Plan-Apochromat 63x/1.40 Oil DIC M27
Z-Stack	73 Slices (2.16 µm)
Channels	2
Scaling (Per Pixel)	0.059 µm X 0.059 µm X 0.030 µm
Image size (Pixels)	1341 X 1115
Image Size (Scaled)	78.85 µm X 65.56 µm
Bit Depth	16 Bit
Image Center Position	X: 97.20 mm, Y: 46.14 mm
Stage Position	X: 97.20 mm, Y: 46.14 mm
ROI Center Offset	X: 0.00 µm, Y: 0.00 µm
Reflector	None
Contrast Method	Fluorescence
Pinhole	1.00 AU / 65 µm | 1.00 AU / 51 µm
LMS MBS	MBS 488/639 & 405/730
LMS SBS	SBS SP 615 | SBS SP 505
Laser Wavelength	639 nm @ 0.3% | 488 nm @ 0.3%
Laser Blanking	Enabled
Scan Mode	Frame
Scan Zoom	1.5
Rotation	0°
Sampling	1.20
Pixel Time	0.26 µs
Frame Time	5.63 s
LSM Scan Speed	11
Scan Direction	Bidirectional
Line Step	1
Averaging	8
Excitation Wavelength	653 | 493
Emission Wavelength	668 | 517
Effective NA	1.4
Detection Wavelength	640 - 732 | 511 - 550
Imaging Device	GaAsP-Pmt3

FIELD	SOURCE-DOCUMENTED VALUE
Detector Type	GaAsP-PMT
Detector Gain	500 V
Detector Offset	0
Detector Digital Gain	1.0
LSM Plus Mode	Filter: 8.1 (3D, Auto) | Filter: 7.7 (3D, Auto)
Profile Definition	Stroke Thickness 1, Normal View, Grid Distance 1
Profile View	X and Y axes were set to Auto - X (Min 0.0 and Max 30.9), Y (Min 0.0 and Max 43793)
Panel A - Single Z-plane (Z	33 of 73) from a confocal acquisition of Rabbit anti-Human ATM.p (Serine 1981) Recombinant Monoclonal, IgG - (BLR031P), detected using Identifyn® SRM Alexa Fluor™ 647 affinity-purified Goat Anti-Rabbit F(ab')□ (H + L). A line profile traverses a single nucleus to define the region used for quantitative analysis of phospho-ATM aggregate formation and the distribution of fluorescence intensity within the nuclear compartment.

SOURCE METHOD

The text below is carried from the preserved Identifyn source record. Typography and pagination have been normalized for this preservation dossier; scientific wording has not been editorially rewritten.

Identifyn Standards for Optical Microscopy Methods™

Identifyn® Primary Antibody

Rabbit anti-Human ATM.p (Serine 1981) Recombinant Monoclonal, IgG - (BLR031P)
Cat ID# PA-RR 000012

Mouse anti-Human H2Ax Monoclonal, IgG1 - (1H1D9/B7)
Cat ID# - PA-MM 000002

Identifyn® Secondary Antibodies

Identifyn® SRM Alexa Fluor™ 647 Affinity Purified Goat Anti-Rabbit, F(ab')□ (H + L)
Cat ID# - SA 000063

Identifyn® SRM Alexa Fluor™ 488 Affinity Purified Donkey Anti-Mouse, F(ab')□ (H + L)
Cat ID# - SA 000019

ATM (ataxia-telangiectasia mutated) is a crucial serine/threonine kinase that plays a central role in the DNA damage response (DDR), particularly in response to DNA double-strand breaks (DSBs). ATM's activation and subsequent phosphorylation cascades are essential for detecting DNA damage and initiating repair processes. Here's a detailed overview of how ATM is activated, its targets, and its role in the DDR:

Activation of ATM

In response to DNA damage, particularly DSBs, ATM is activated through a series of events:

Detection of DNA Breaks: ATM can sense DNA breaks by associating with the MRN complex (MRE11, RAD50, and NBS1). This complex recognizes DSBs, leading to ATM's recruitment to the damaged site.

Autophosphorylation: Upon detection of DNA damage, ATM autophosphorylates at serine 1981 (S1981), thereby activating it. This phosphorylation event is critical for ATM's kinase activity and its ability to phosphorylate downstream targets.

Dimer-to-Monomer Transition: In its inactive form, ATM is a dimer. It transitions to an active monomeric state upon activation, allowing it to interact with and phosphorylate various downstream proteins.

Phosphorylation Targets of ATM
Once activated, ATM phosphorylates many proteins involved in the DNA damage response, cell cycle regulation, and apoptosis. Here are some critical targets of ATM:

CHK2: ATM phosphorylates CHK2, a cell cycle checkpoint control kinase. This phosphorylation helps to halt the cell cycle, allowing time for DNA repair.

p53: ATM phosphorylates p53, activating this tumor suppressor, leading to cell cycle arrest or apoptosis if the damage is irreparable.

H2AX: ATM phosphorylates histone H2AX, forming γ-H2AX, a marker of DNA damage. This modification helps signal the presence of DSBs and recruit DNA repair machinery.

BRCA1: ATM's phosphorylation of BRCA1 is critical for homologous recombination, a key DNA repair pathway for DSBs.

NBS1: As part of the MRN complex, NBS1 phosphorylation by ATM enhances the complex's DNA repair functions.

53BP1: ATM phosphorylation of 53BP1 helps recruit this protein to sites of DSBs, thereby guiding repair pathways such as non-homologous end joining (NHEJ).

Role of ATM Phosphorylation in DNA Repair

ATM-mediated phosphorylation plays a central role in coordinating the DNA damage response:
Signal Propagation: Phosphorylation cascades initiated by ATM amplify the signal in response to DNA damage, ensuring an efficient response.

Recruitment of Repair Machinery: Phosphorylation of specific proteins helps recruit DNA repair complexes to the sites of DNA damage.

Cell Cycle Regulation: ATM activation can lead to cell cycle checkpoints, preventing cells with damaged DNA from dividing.

Apoptosis: If the DNA damage is too severe to repair, ATM's activation can lead to apoptosis, preventing the propagation of damaged cells

ATM's phosphorylation in response to DNA damage is crucial for detecting DNA double-strand breaks and coordinating the DNA damage response. By phosphorylating a range of critical proteins, ATM orchestrates a complex signaling network that facilitates DNA repair, cell cycle regulation, and apoptosis, thereby maintaining genomic stability.

Method

HeLa cells were grown on acid-etched #1.5H cover glass to ~50% confluency, DNA damage was induced by treatment with 2 µM Etoposide-spiked complete growth media for 12 hours, followed by -20 °C methanol fixation and blocking with Thermo Fisher Fish Serum Blocker (cat#37527X3). The primary antibody, Rabbit anti-Human ATM.p (Serine 1981) Recombinant Monoclonal, IgG - (BLR031P), was incubated at room temperature for 1 hour at a 1:250 dilution. Cells were washed 3X in PBS. Identifyn® SRM Alexa Fluor™ 647 Affinity Purified Goat Anti-Rabbit, F(ab')□ (H + L) was incubated at room temperature for 1 hour at a dilution of 1:1000. Cells were washed 5X in PBS.

The second primary antibody, Mouse anti-Human H2Ax Monoclonal, IgG1 - (1H1D9/B7), was then incubated for 1 hour at room temperature at a dilution of 1:250. Cells were washed 3X in PBS.
Identifyn® SRM Alexa Fluor™ 488 Affinity Purified Donkey Anti-Mouse, F(ab')□ (H + L) was incubated for 1 hour at room temperature at a dilution of 1:1000. Cells were washed 5X in PBS and mounted using ProLong™ Diamond Antifade Mountant with DAPI cat#P36962.

Microscope

Zeiss LSM980 Confocal with NIR Detection, Axio Observer.Z1/7, using a Plan-Apochromat 63x/1.40 Oil DIC M27, was used with the following parameters for each dye:

Z Stack - (3D) - Panel A, Showing Z-Plane 33 of 73

Z-Stack = 73 Slices (2.16 µm)

Channels = 2
Scaling (Per Pixel) = 0.059 µm X 0.059 µm X 0.030 µm
Image size (Pixels) = 1341 X 1115
Image Size (Scaled) = 78.85 µm X 65.56 µm
Bit Depth = 16 Bit
Image Center Position = X: 97.20 mm, Y: 46.14 mm
Stage Position = X: 97.20 mm, Y: 46.14 mm
ROI Center Offset = X: 0.00 µm, Y: 0.00 µm

647 -

Reflector = None
Contrast Method = Fluorescence
Pinhole = 1.00 AU / 65 µm
LMS MBS = MBS 488/639 & 405/730
LMS SBS = SBS SP 615
Laser Wavelength = 639 nm @ 0.3%
Laser Blanking = Enabled
Scan Mode = Frame
Scan Zoom = 1.5
Rotation = 0°
Sampling = 1.20
Pixel Time = 0.26 µs
Frame Time = 5.63 s
LSM Scan Speed = 11
Scan Direction = Bidirectional
Line Step = 1
Averaging = 8
Excitation Wavelength = 653
Emission Wavelength = 668
Effective NA = 1.4
Detection Wavelength = 640 - 732
Imaging Device = GaAsP-Pmt3
Detector Type = GaAsP-PMT
Detector Gain = 500 V
Detector Offset = 0
Detector Digital Gain = 1.0
LSM Plus Mode = Filter: 8.1 (3D, Auto)

488 - Acquired but Not Shown in Data Analysis

Reflector = None
Contrast Method = Fluorescence
Pinhole = 1.00 AU / 51 µm
LMS MBS = MBS 488/639 & 405/730
LMS SBS = SBS SP 505
Laser Wavelength = 488 nm @ 0.3%
Laser Blanking = Enabled
Scan Mode = Frame
Scan Zoom = 1.5
Rotation = 0°
Sampling = 1.20
Pixel Time = 0.26 µs
Frame Time = 5.63 s
LSM Scan Speed = 11
Scan Direction = Bidirectional
Line Step = 1
Averaging = 8
Excitation Wavelength = 493
Emission Wavelength = 517
Effective NA = 1.4
Detection Wavelength = 511 - 550
Imaging Device = GaAsP-Pmt3
Detector Type = GaAsP-PMT
Detector Gain = 500 V
Detector Offset = 0
Detector Digital Gain = 1.0
LSM Plus Mode = Filter: 7.7 (3D, Auto)

Profile View Display - Panels A & B

Profile Definition = Stroke Thickness 1, Normal View, Grid Distance 1

Profile View = X and Y axes were set to Auto - X (Min 0.0 and Max 30.9), Y (Min 0.0 and Max 43793)

Measured at Z-plane 33 of 73

Zen Acquisition Info Tab - Panel C

Shown are the acquisition parameters for the 647 channel (phospho-ATM) collected using the 639 nm laser at 0.3% power. Scan zoom, scan speed, and line-averaging settings are provided to ensure the transparency and reproducibility of line-profile measurements.

Summary

Panel A - Single Z-plane (Z = 33 of 73) from a confocal acquisition of Rabbit anti-Human ATM.p (Serine 1981) Recombinant Monoclonal, IgG - (BLR031P), detected using Identifyn® SRM Alexa Fluor™ 647 affinity-purified Goat Anti-Rabbit F(ab')□ (H + L). A line profile traverses a single nucleus to define the region used for quantitative analysis of phospho-ATM aggregate formation and the distribution of fluorescence intensity within the nuclear compartment.

Panel B - Corresponding line-profile analysis demonstrates three prominent phospho-ATM aggregate measurements of 41,708.00, 38,229.00, and 29,400.00 A.U., respectively, indicating substantial local enrichment of phospho-ATM

signal following etoposide-induced DNA damage. These intensity peaks are consistent with recruitment and concentration of activated ATM signaling within DNA damage-associated nuclear foci. At confocal resolution, these structures appear as discrete punctate aggregates; however, higher-resolution imaging modalities demonstrate that such apparent foci likely represent clustered signaling assemblies or multi-component repair-associated microenvironments rather than singular molecular structures.

Biologically, ATM phosphorylation represents a central upstream event in the DNA damage response following induction of DNA double-strand breaks. Activated phospho-ATM coordinates checkpoint signaling, chromatin remodeling, and recruitment of downstream repair factors, including phosphorylation of H2Ax into γH2AX within damage-associated chromatin territories. The observed focal enrichment is therefore consistent with localized activation of ATM-mediated DNA damage signaling and organization of repair-associated nuclear domains following genotoxic stress.

Panel C - Zeiss ZEN acquisition settings demonstrate that the phospho-ATM signal was acquired with the 639 nm laser at only 0.3% input power, supporting the conclusion that the measured fluorescent intensities reflect true biological enrichment and aggregate formation rather than detector saturation or excessive excitation conditions.

Image Correction

The phospho-ATM (Serine 1981) channel (647) was pseudocolored white to enhance visual contrast.

Image by J.K. Bennett
Image Analysis and Data Presentation by B.T. Bennett

SOURCE PROVENANCE

Catalog	PA-RR-000012
Stage	Confocal
Instrument	ZEISS LSM 980
Microscope configuration	Zeiss LSM980 Confocal with NIR Detection, Axio Observer.Z1/7, using a Plan-Apochromat 63x/1.40 Oil DIC M27, was used with the following parameters for each dye:
Structured source metadata values	46
Metadata source	PRESERVED_SOURCE_METHOD_PDF_TEXT
Cell model	HeLa
Image SHA-256	DC68943B3BB69566CDC621FFFE36D983DDEECEEBB69CEC2F13A071400F5BC3CF
Method PDF SHA-256	6A9C9717B4F4BA77A019838BE16ECB01FDA03A0B2444726863F311D23EEF1831

ORIGINAL IMAGE EVIDENCE / AIRYSCAN

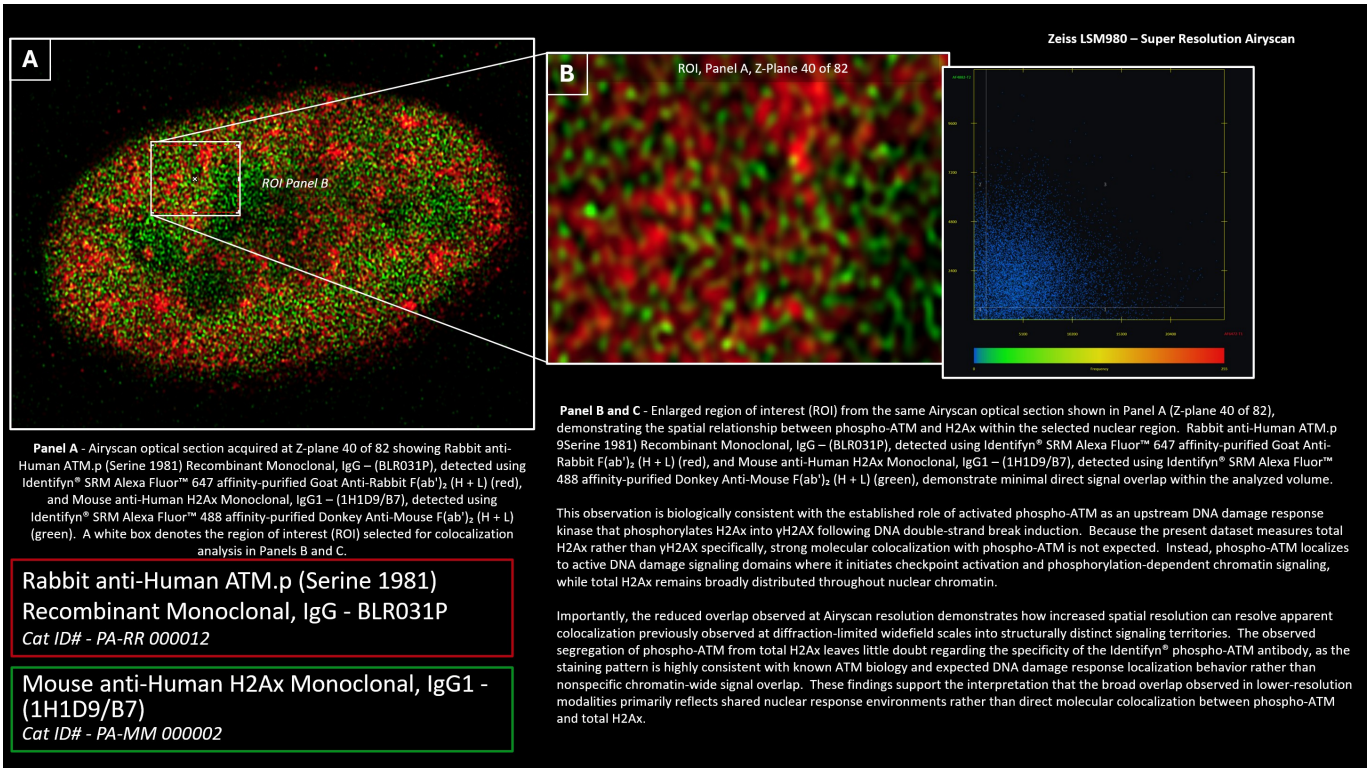

Panel A - Airyscan optical section acquired at Z-plane 40 of 82 showing Rabbit anti-Human ATM.p (Serine 1981) Recombinant Monoclonal, IgG – (BLR031P), detected using Identifyn® SRM Alexa Fluor™ 647 affinity-purified Goat Anti-Rabbit F(ab')$_2$ (H + L) (red), and Mouse anti-Human H2Ax Monoclonal, IgG1 – (1H1D9/B7), detected using Identifyn® SRM Alexa Fluor™ 488 affinity-purified Donkey Anti-Mouse F(ab')$_2$ (H + L) (green). A white box denotes the region of interest (ROI) selected for colocalization analysis in Panels B and C.

Rabbit anti-Human ATM.p (Serine 1981) Recombinant Monoclonal, IgG - BLR031P
Cat ID# - PA-RR 000012

Mouse anti-Human H2Ax Monoclonal, IgG1 - (1H1D9/B7)
Cat ID# - PA-MM 000002

Panel B and C - Enlarged region of interest (ROI) from the same Airyscan optical section shown in Panel A (Z-plane 40 of 82), demonstrating the spatial relationship between phospho-ATM and H2Ax within the selected nuclear region. Rabbit anti-Human ATM.p 9Serine 1981) Recombinant Monoclonal, IgG – (BLR031P), detected using Identifyn® SRM Alexa Fluor™ 647 affinity-purified Goat Anti-Rabbit F(ab')$_2$ (H + L) (red), and Mouse anti-Human H2Ax Monoclonal, IgG1 – (1H1D9/B7), detected using Identifyn® SRM Alexa Fluor™ 488 affinity-purified Donkey Anti-Mouse F(ab')$_2$ (H + L) (green), demonstrate minimal direct signal overlap within the analyzed volume.

This observation is biologically consistent with the established role of activated phospho-ATM as an upstream DNA damage response kinase that phosphorylates H2Ax into γH2AX following DNA double-strand break induction. Because the present dataset measures total H2Ax rather than γH2AX specifically, strong molecular colocalization with phospho-ATM is not expected. Instead, phospho-ATM localizes to active DNA damage signaling domains where it initiates checkpoint activation and phosphorylation-dependent chromatin signaling, while total H2Ax remains broadly distributed throughout nuclear chromatin.

Importantly, the reduced overlap observed at Airyscan resolution demonstrates how increased spatial resolution can resolve apparent colocalization previously observed at diffraction-limited widefield scales into structurally distinct signaling territories. The observed segregation of phospho-ATM from total H2Ax leaves little doubt regarding the specificity of the Identifyn® phospho-ATM antibody, as the staining pattern is highly consistent with known ATM biology and expected DNA damage response localization behavior rather than nonspecific chromatin-wide signal overlap. These findings support the interpretation that the broad overlap observed in lower-resolution modalities primarily reflects shared nuclear response environments rather than direct molecular colocalization between phospho-ATM and total H2Ax.

EVIDENCE TIER	Airyscan
INSTRUMENT	ZEISS LSM 980
CELL MODEL	HeLa
DETECTED DYES	405/DAPI; 488; 647
METADATA VALUES	46

STRUCTURED ACQUISITION METADATA / AIRYSCAN

The values below were deterministically extracted from the preserved Identifyn method PDF text. They remain source-documented metadata, not new BENNETT measurements.

FIELD	SOURCE-DOCUMENTED VALUE
Platform / configuration	Zeiss LSM980 Confocal with NIR Detection, Axio Observer.Z1/7, using a Plan-Apochromat 63x/1.40 Oil DIC M27, was used with the following parameters for each dye:
Objective	Plan-Apochromat 63x/1.40 Oil DIC M27
Z-Stack	82 Slices (2.43 µm)
Channels	2
Scaling (Per Pixel)	0.03529 µm X 0.03529 µm X 0.03000 µm
Image Size (Pixels)	945 X 703 | 154 X 118
Image Size (Scaled)	33.34 µm X 24.81 µm | 5.43 µm X 4.16 µm
Bit Depth	16 Bit
Image Center Position	X: 92.76 mm, Y: 50.17 mm
Stage Position	X: 92.76 mm, Y: 50.17 mm
ROI Center Offset	X: 0.00 µm, Y: 0.00 µm
Reflector	None
Contrast Method	Fluorescence
Pinhole	5.00 AU / 328 µm | 5.00 AU / 250 µm
LMS MBS	MBS 488/639 & 405/730
LMS SBS	SBS LP 640 | SBS SP 550
Laser Wavelength	639 nm @ 0.40% | 488 nm @ 0.5%
Laser Blanking	Enabled
Scan Mode	Frame
Scan Zoom	1.9
Rotation	0°
Sampling	2.00
Pixel Time	1.04 µs
Frame Time	19.77 s
LSM Scan Speed	6
Scan Direction	Bidirectional
Line Step	1
Averaging	4
Excitation Wavelength	653 | 493
Emission Wavelength	668 | 517
Effective NA	1.4
Detection Wavelength	643 - 735 | 499 - 548
Imaging Device	Airyscan

FIELD	SOURCE-DOCUMENTED VALUE
Detector Type	GaAsP-PMT
Detector Gain	800 V
Detector Offset	0
Detector Digital Gain	1.0
Airyscan Mode	Super Resolution: 9.8 (3D, Auto) | Super Resolution: 9.5 (3D, Auto)
Image Measurement	Entire Field of Panel B

SOURCE METHOD

The text below is carried from the preserved Identifyn source record. Typography and pagination have been normalized for this preservation dossier; scientific wording has not been editorially rewritten.

Identifyn Standards for Optical Microscopy Methods™

Identifyn® Primary Antibody

Rabbit anti-Human ATM.p (Serine 1981) Recombinant Monoclonal, IgG - (BLR031P)
Cat ID# PA-RR 000012

Mouse anti-Human H2Ax Monoclonal, IgG1 - (1H1D9/B7)
Cat ID# - PA-MM 000002

Identifyn® Secondary Antibodies

Identifyn® SRM Alexa Fluor™ 647 Affinity Purified Goat Anti-Rabbit, F(ab')□ (H + L)
Cat ID# - SA 000063

Identifyn® SRM Alexa Fluor™ 488 Affinity Purified Donkey Anti-Mouse, F(ab')□ (H + L)
Cat ID# - SA 000019

ATM (ataxia-telangiectasia mutated) is a crucial serine/threonine kinase that plays a central role in the DNA damage response (DDR), particularly in response to DNA double-strand breaks (DSBs). ATM's activation and subsequent phosphorylation cascades are essential for detecting DNA damage and initiating repair processes. Here's a detailed overview of how ATM is activated, its targets, and its role in the DDR:

Activation of ATM

In response to DNA damage, particularly DSBs, ATM is activated through a series of events:

Detection of DNA Breaks: ATM can sense DNA breaks by associating with the MRN complex (MRE11, RAD50, and NBS1). This complex recognizes DSBs, leading to ATM's recruitment to the damaged site.

Autophosphorylation: Upon detection of DNA damage, ATM autophosphorylates at serine 1981 (S1981), thereby activating it. This phosphorylation event is critical for ATM's kinase activity and its ability to phosphorylate downstream targets.

Dimer-to-Monomer Transition: In its inactive form, ATM is a dimer. It transitions to an active monomeric state upon activation, allowing it to interact with and phosphorylate various downstream proteins.

Phosphorylation Targets of ATM
Once activated, ATM phosphorylates many proteins involved in the DNA damage response, cell cycle regulation, and apoptosis. Here are some critical targets of ATM:

CHK2: ATM phosphorylates CHK2, a cell cycle checkpoint control kinase. This phosphorylation helps to halt the cell cycle, allowing time for DNA repair.

p53: ATM phosphorylates p53, activating this tumor suppressor, leading to cell cycle arrest or apoptosis if the damage is irreparable.

H2AX: ATM phosphorylates histone H2AX, forming γ-H2AX, a marker of DNA damage. This modification helps signal the presence of DSBs and recruit DNA repair machinery.

BRCA1: ATM's phosphorylation of BRCA1 is critical for homologous recombination, a key DNA repair pathway for DSBs.

NBS1: As part of the MRN complex, NBS1 phosphorylation by ATM enhances the complex's DNA repair functions.

53BP1: ATM phosphorylation of 53BP1 helps recruit this protein to sites of DSBs, thereby guiding repair pathways such as non-homologous end joining (NHEJ).

Role of ATM Phosphorylation in DNA Repair

ATM-mediated phosphorylation plays a central role in coordinating the DNA damage response:
Signal Propagation: Phosphorylation cascades initiated by ATM amplify the signal in response to DNA damage, ensuring an efficient response.

Recruitment of Repair Machinery: Phosphorylation of specific proteins helps recruit DNA repair complexes to the sites of DNA damage.

Cell Cycle Regulation: ATM activation can lead to cell cycle checkpoints, preventing cells with damaged DNA from dividing.

Apoptosis: If the DNA damage is too severe to repair, ATM's activation can lead to apoptosis, preventing the propagation of damaged cells

ATM's phosphorylation in response to DNA damage is crucial for detecting DNA double-strand breaks and coordinating the DNA damage response. By phosphorylating a range of critical proteins, ATM orchestrates a complex signaling network that facilitates DNA repair, cell cycle regulation, and apoptosis, thereby maintaining genomic stability.

Method

HeLa cells were grown on acid-etched #1.5H cover glass to ~50% confluency, DNA damage was induced by treatment with 2 µM Etoposide-spiked complete growth media for 12 hours, followed by -20 °C methanol fixation and blocking with Thermo Fisher Fish Serum Blocker (cat#37527X3). The primary antibody, Rabbit anti-Human ATM.p (Serine 1981) Recombinant Monoclonal, IgG - (BLR031P), was incubated at room temperature for 1 hour at a 1:250 dilution. Cells were washed 3X in PBS. Identifyn® SRM Alexa Fluor™ 647 Affinity Purified Goat Anti-Rabbit, F(ab')□ (H + L) was incubated at room temperature for 1 hour at a dilution of 1:1000. Cells were washed 5X in PBS.

The second primary antibody, Mouse anti-Human H2Ax Monoclonal, IgG1 - (1H1D9/B7), was then incubated for 1 hour at room temperature at a dilution of 1:250. Cells were washed 3X in PBS.
Identifyn® SRM Alexa Fluor™ 488 Affinity Purified Donkey Anti-Mouse, F(ab')□ (H + L) was incubated for 1 hour at room temperature at a dilution of 1:1000. Cells were washed 5X in PBS and mounted using ProLong™ Diamond Antifade Mountant with DAPI cat#P36962.

Microscope

Zeiss LSM980 Confocal with NIR Detection, Axio Observer.Z1/7, using a Plan-Apochromat 63x/1.40 Oil DIC M27, was used with the following parameters for each dye:

Z Stack - (3D) - Panel A, Z-Plane 40 of 82

Z-Stack = 82 Slices (2.43 µm)

Channels = 2
Scaling (Per Pixel) = 35.29 nm X 35.29 nm X 30.00 nm
Image Size (Pixels) = 945 X 703
Image Size (Scaled) = 33.34 µm X 24.81 µm
Bit Depth = 16 Bit
Image Center Position = X: 92.76 mm, Y: 50.17 mm
Stage Position = X: 92.76 mm, Y: 50.17 mm
ROI Center Offset = X: 0.00 µm, Y: 0.00 µm

Z Stack - (3D) - Panels B and C, Colocalization Measurement, same Z-Plane.

Z-Stack = 82 Slices (2.43 µm)

Channels = 2
Scaling (Per Pixel) = 35.29 nm X 35.29 nm X 30.00 nm
Image Size (Pixels) = 154 X 118
Image Size (Scaled) = 5.43 µm X 4.16 µm
Bit Depth = 16 Bit
Image Center Position = X: 92.76 mm, Y: 50.17 mm
Stage Position = X: 92.76 mm, Y: 50.17 mm
ROI Center Offset = X: 0.00 µm, Y: 0.00 µm

647 -

Reflector = None
Contrast Method = Fluorescence
Pinhole = 5.00 AU / 328 µm
LMS MBS = MBS 488/639 & 405/730
LMS SBS = SBS LP 640
Laser Wavelength = 639 nm @ 0.40%
Laser Blanking = Enabled
Scan Mode = Frame
Scan Zoom = 1.9
Rotation = 0°
Sampling = 2.00
Pixel Time = 1.04 µs
Frame Time = 19.77 s
LSM Scan Speed = 6
Scan Direction = Bidirectional
Line Step = 1
Averaging = 4
Excitation Wavelength = 653
Emission Wavelength = 668
Effective NA = 1.4
Detection Wavelength = 643 - 735
Imaging Device = Airyscan
Detector Type = GaAsP-PMT
Detector Gain = 800 V
Detector Offset = 0
Detector Digital Gain = 1.0
Airyscan Mode = Super Resolution: 9.8 (3D, Auto)

488 -

Reflector = None
Contrast Method = Fluorescence
Pinhole = 5.00 AU / 250 µm
LMS MBS = MBS 488/639 & 405/730
LMS SBS = SBS SP 550
Laser Wavelength = 488 nm @ 0.5%
Laser Blanking = Enabled
Scan Mode = Frame
Scan Zoom = 1.9
Rotation = 0°
Sampling = 2.00
Pixel Time = 1.04 µs
Frame Time = 19.77 s
LSM Scan Speed = 6
Scan Direction = Bidirectional
Line Step = 1
Averaging = 4
Excitation Wavelength = 493
Emission Wavelength = 517
Effective NA = 1.4
Detection Wavelength = 499 - 548
Imaging Device = Airyscan
Detector Type = GaAsP-PMT
Detector Gain = 800 V
Detector Offset = 0
Detector Digital Gain = 1.0
Airyscan Mode = Super Resolution: 9.5 (3D, Auto)

2-Dimensional View - Panel A

Airyscan optical section acquired at Z-plane 40 of 82 showing Rabbit anti-Human ATM.p (Serine 1981) Recombinant Monoclonal, IgG - (BLR031P), detected using Identifyn® SRM Alexa Fluor™ 647 affinity-purified Goat Anti-Rabbit F(ab')□ (H + L) (red), and Mouse anti-Human H2Ax Monoclonal, IgG1 - (1H1D9/B7), detected using Identifyn® SRM Alexa Fluor™ 488 affinity-purified Donkey Anti-Mouse F(ab')□ (H + L) (green). A white box denotes the region of interest (ROI) selected for colocalization analysis in Panels B and C.

Colocalization View - Panels B and C

Horizontal Axis - AF647, Threshold 4521, Range Auto
Vertical Axis - AF488, Threshold 12040, Range Auto

Image Measurement = Entire Field of Panel B

Colocalization analysis of phospho-ATM (X-axis) and H2Ax (Y-axis) was performed across the entire image acquisition.

Phospho-ATM shows a lack of colocalization with H2Ax, consistent with the known biology of phospho-ATM signaling and total H2Ax distribution.

Summary

Panel A shows an Airyscan optical section acquired at Z-plane 40 of 82 demonstrating Rabbit anti-Human ATM.p (Serine 1981) Recombinant Monoclonal, IgG - (BLR031P), detected using Identifyn® SRM Alexa Fluor™ 647 affinity-purified Goat Anti-Rabbit F(ab')□ (H + L) (red), and Mouse anti-Human H2Ax Monoclonal, IgG1 - (1H1D9/B7), detected using Identifyn® SRM Alexa Fluor™ 488 affinity-purified Donkey Anti-Mouse F(ab')□ (H + L) (green). A white box denotes the region of interest (ROI) selected for colocalization analysis in Panels B and C.

Panel B presents an enlarged ROI from the same Airyscan optical section shown in Panel A, demonstrating the spatial relationship between phospho-ATM and H2Ax within the selected nuclear region. Minimal direct signal overlap is observed between phospho-ATM and total H2Ax within the analyzed volume. This finding is biologically consistent with the established role of activated phospho-ATM as an upstream DNA damage response kinase responsible for phosphorylation of H2Ax into γH2AX following induction of DNA double-strand breaks. Because the present dataset measures total H2Ax rather than γH2AX specifically, strong molecular colocalization with phospho-ATM is not expected. Instead, phospho-ATM localizes to active DNA damage signaling domains and checkpoint-associated repair territories, while total H2Ax remains broadly distributed throughout chromatin.

Importantly, this dataset functions as a biological pressure test for the Identifyn® phospho-ATM antibody under super-resolution conditions. If the antibody lacked specificity, substantial nonspecific overlap with broadly distributed H2Ax chromatin signal would be expected. Instead, the reduced overlap observed at Airyscan resolution demonstrates that increased spatial resolution resolves the apparent colocalization previously observed at diffraction-limited widefield scales into structurally distinct signaling territories. The observed segregation of phospho-ATM from total H2Ax strongly supports the specificity of the Identifyn® phospho-ATM antibody, as the staining pattern closely matches the expected biological behavior of activated ATM signaling rather than nonspecific chromatin-wide overlap. Collectively, these findings support the interpretation that the broad overlap observed in lower-resolution imaging modalities primarily reflects shared DNA-damage-associated nuclear environments rather than direct molecular colocalization between phospho-ATM and total H2Ax.

Image Correction

NONE

Image by J.K. Bennett
Image Analysis and Data Presentation by B.T. Bennett

SOURCE PROVENANCE

Catalog	PA-RR-000012
Stage	Airyscan
Instrument	ZEISS LSM 980
Microscope configuration	Zeiss LSM980 Confocal with NIR Detection, Axio Observer.Z1/7, using a Plan-Apochromat 63x/1.40 Oil DIC M27, was used with the following parameters for each dye:
Structured source metadata values	46
Metadata source	PRESERVED_SOURCE_METHOD_PDF_TEXT
Cell model	HeLa

SOURCE PROVENANCE

Image SHA-256	A0E59462F8518A20E6D3F5F68F219C3D8ED49F2DCC75693308DFA3D73D78D202
Method PDF SHA-256	00478FF006FBC4C1DF89982ED72542768B27A2AC00A36CE519857244E9D96E90

ORIGINAL IMAGE EVIDENCE / SIM

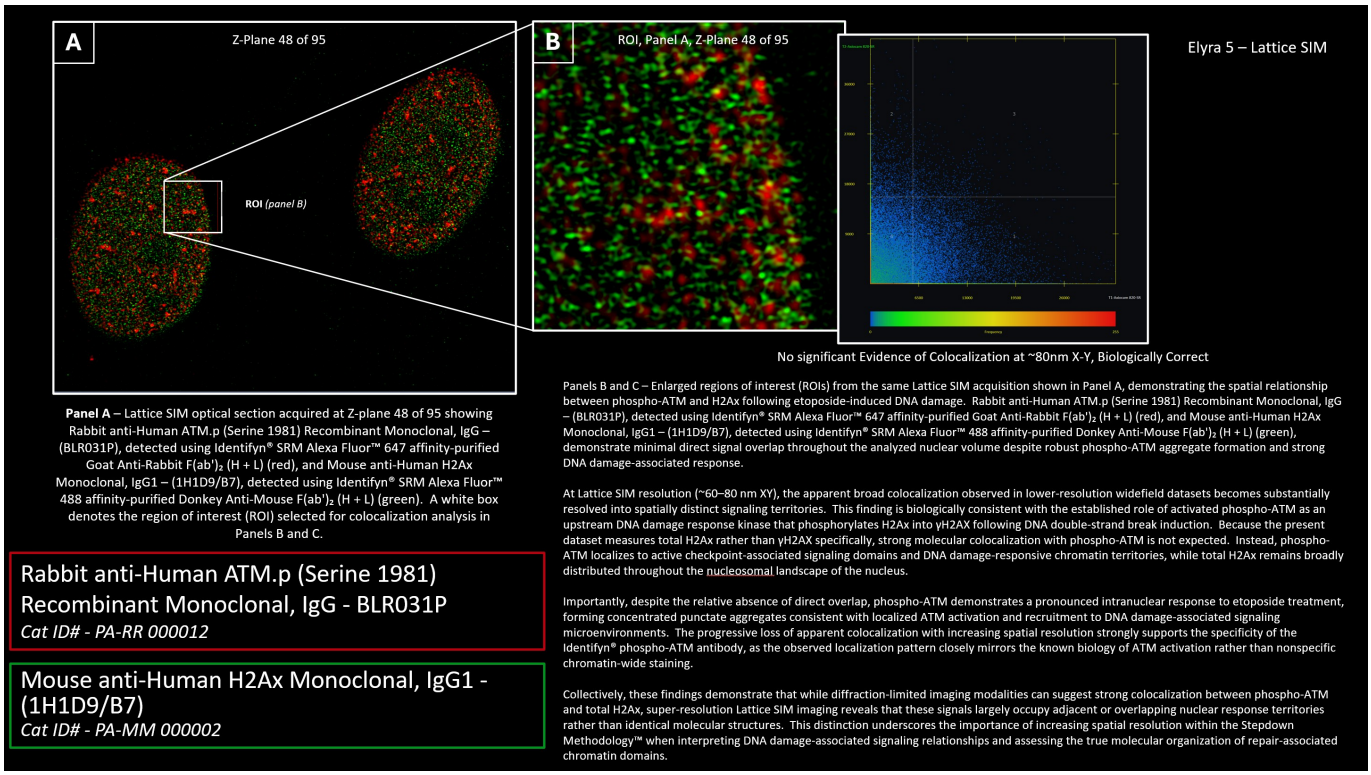

EVIDENCE TIER	SIM
INSTRUMENT	ZEISS Elyra
CELL MODEL	HeLa
DETECTED DYES	405/DAPI; 488; 647
METADATA VALUES	50

STRUCTURED ACQUISITION METADATA / SIM

The values below were deterministically extracted from the preserved Identifyn method PDF text. They remain source-documented metadata, not new BENNETT measurements.

FIELD	SOURCE-DOCUMENTED VALUE
Platform / configuration	Zeiss Elyra 5 Lattice SIM, AxioObserver.Z1/ 7 using Plan-Apochromat 63X/1.40 oil DIC M27, 1X Tubelens, was used with the following parameters for each dye:
Objective	Plan-Apochromat 63X/1.40 oil DIC M27
Z-Stack	95 Slices (2.82 µm)
Channels	2
Scaling (Per Pixel)	0.02111 µm X 0.02111 µm X 0.03000 µm
Image Size (Pixels)	3155 X 2512 | 365 X 360
Image Size (Scaled)	66.61 µm X 53.03 µm | 7.71 µm X 7.60 µm
Bit Depth	16 Bit
Image Center Position	X: 57.77 mm, Y: 35.27 mm
Stage Position	X: 57.77 mm, Y: 35.27 mm
ROI Center Offset	X: 0.00 µm, Y: 0.00 µm
Reflectors	SR HE LBF 405/488/561/642
Beam Splitter	405, 488, 561, 642
Filter Excitation Wavelength	200 - 405, 200 - 488, 200 - 561, 200 - 642
Filter Emission Wavelength	419 - 470, 503 - 546, 576 - 617, 657 - 800
Contrast Method	Fluorescence
Illumination Wavelength	640 | 488
Channel Name	T1-Axiocam 820 | T2-Axiocam 820
Excitation Wavelength	640 | 488
Emission Wavelength	729 | 525
Effective NA	1.4
Detection Wavelength	419 - 470, 503 - 546, 576 - 617, 657 - 800
Imaging Device	Axiocam 820
Camera Adapter	1X
Exposure Time	100 ms | 120 ms
Depth of Focus	1.13 µm | 0.81 µm
Binning Mode	2,2
Laser Wavelength	640 nm @ 1.0% | 488 nm @ 1.00%
Frame Time	1.33 s | 1.59 s
Scan Direction	Unidirectional
Grating	36.5 µm grating | 27.5 µm grating
Processing Dimension	3D
Result Sampling	4

FIELD	SOURCE-DOCUMENTED VALUE
Process Sampling	N/A
Algorithm	SIM
SIM Settings	Standard
Auto Sharpness	On
Sharpness	11.0018 (647), 11.2478 (488)
Fitting	Fast Fit
Normalization	Auto
Image Measurement	Entire Field of Panel B

SOURCE METHOD

The text below is carried from the preserved Identifyn source record. Typography and pagination have been normalized for this preservation dossier; scientific wording has not been editorially rewritten.

Identifyn Standards for Optical Microscopy Methods™

Identifyn® Primary Antibody

Rabbit anti-Human ATM.p (Serine 1981) Recombinant Monoclonal, IgG - (BLR031P)
Cat ID# PA-RR 000012

Mouse anti-Human H2Ax Monoclonal, IgG1 - (1H1D9/B7)
Cat ID# - PA-MM 000002

Identifyn® Secondary Antibodies

Identifyn® SRM Alexa Fluor™ 647 Affinity Purified Goat Anti-Rabbit, F(ab')□ (H + L)
Cat ID# - SA 000063

Identifyn® SRM Alexa Fluor™ 488 Affinity Purified Donkey Anti-Mouse, F(ab')□ (H + L)
Cat ID# - SA 000019

ATM (ataxia-telangiectasia mutated) is a crucial serine/threonine kinase that plays a central role in the DNA damage response (DDR), particularly in response to DNA double-strand breaks (DSBs). ATM's activation and subsequent phosphorylation cascades are essential for detecting DNA damage and initiating repair processes. Here's a detailed overview of how ATM is activated, its targets, and its role in the DDR:

Activation of ATM

In response to DNA damage, particularly DSBs, ATM is activated through a series of events:

Detection of DNA Breaks: ATM can sense DNA breaks by associating with the MRN complex (MRE11, RAD50, and NBS1). This complex recognizes DSBs, leading to ATM's recruitment to the damaged site.

Autophosphorylation: Upon detection of DNA damage, ATM autophosphorylates at serine 1981 (S1981), thereby activating it. This phosphorylation event is critical for ATM's kinase activity and its ability to phosphorylate downstream targets.

Dimer-to-Monomer Transition: In its inactive form, ATM is a dimer. It transitions to an active monomeric state upon activation, allowing it to interact with and phosphorylate various downstream proteins.

Phosphorylation Targets of ATM
Once activated, ATM phosphorylates many proteins involved in the DNA damage response, cell cycle regulation, and apoptosis. Here are some critical targets of ATM:

CHK2: ATM phosphorylates CHK2, a cell cycle checkpoint control kinase. This phosphorylation helps to halt the cell cycle, allowing time for DNA repair.

p53: ATM phosphorylates p53, activating this tumor suppressor, leading to cell cycle arrest or apoptosis if the damage is irreparable.

H2AX: ATM phosphorylates histone H2AX, forming γ-H2AX, a marker of DNA damage. This modification helps signal the presence of DSBs and recruit DNA repair machinery.

BRCA1: ATM's phosphorylation of BRCA1 is critical for homologous recombination, a key DNA repair pathway for DSBs.

NBS1: As part of the MRN complex, NBS1 phosphorylation by ATM enhances the complex's DNA repair functions.

53BP1: ATM phosphorylation of 53BP1 helps recruit this protein to sites of DSBs, thereby guiding repair pathways such as non-homologous end joining (NHEJ).

Role of ATM Phosphorylation in DNA Repair

ATM-mediated phosphorylation plays a central role in coordinating the DNA damage response:
Signal Propagation: Phosphorylation cascades initiated by ATM amplify the signal in response to DNA damage, ensuring an efficient response.

Recruitment of Repair Machinery: Phosphorylation of specific proteins helps recruit DNA repair complexes to the sites of DNA damage.

Cell Cycle Regulation: ATM activation can lead to cell cycle checkpoints, preventing cells with damaged DNA from dividing.

Apoptosis: If the DNA damage is too severe to repair, ATM's activation can lead to apoptosis, preventing the propagation of damaged cells

ATM's phosphorylation in response to DNA damage is crucial for detecting DNA double-strand breaks and coordinating the DNA damage response. By phosphorylating a range of critical proteins, ATM orchestrates a complex signaling network that facilitates DNA repair, cell cycle regulation, and apoptosis, thereby maintaining genomic stability.

Method

HeLa cells were grown on acid-etched #1.5H cover glass to ~50% confluency, DNA damage was induced by treatment with 2 µM Etoposide-spiked complete growth media for 12 hours, followed by -20 °C methanol fixation and blocking with Thermo Fisher Fish Serum Blocker (cat#37527X3). The primary antibody, Rabbit anti-Human ATM.p (Serine 1981) Recombinant Monoclonal, IgG - (BLR031P), was incubated at room temperature for 1 hour at a 1:250 dilution. Cells were washed 3X in PBS. Identifyn® SRM Alexa Fluor™ 647 Affinity Purified Goat Anti-Rabbit, F(ab')□ (H + L) was incubated at room temperature for 1 hour at a dilution of 1:1000. Cells were washed 5X in PBS.

The second primary antibody, Mouse anti-Human H2Ax Monoclonal, IgG1 - (1H1D9/B7), was then incubated for 1 hour at room temperature at a dilution of 1:250. Cells were washed 3X in PBS.
Identifyn® SRM Alexa Fluor™ 488 Affinity Purified Donkey Anti-Mouse, F(ab')□ (H + L) was incubated for 1 hour at room temperature at a dilution of 1:1000. Cells were washed 5X in PBS and mounted using ProLong™ Diamond Antifade Mountant with DAPI cat#P36962.

Microscope

Zeiss Elyra 5 Lattice SIM, AxioObserver.Z1/ 7 using Plan-Apochromat 63X/1.40 oil DIC M27, 1X Tubelens, was used with the following parameters for each dye:

Z Stack - (3D) - Panel A, Z-Plane 48 of 95

Z-Stack = 95 Slices (2.82 µm)

Channels = 2
Scaling (Per Pixel) = 21.11 nm X 21.11 nm X 30.00 nm
Image Size (Pixels) = 3155 X 2512
Image Size (Scaled) = 66.61 µm X 53.03 µm
Bit Depth = 16 Bit
Image Center Position = X: 57.77 mm, Y: 35.27 mm
Stage Position = X: 57.77 mm, Y: 35.27 mm
ROI Center Offset = X: 0.00 µm, Y: 0.00 µm

Z Stack - (3D) - Panels B and C, Colocalization Measurement, same Z-Plane.

Z-Stack = 95 Slices (2.82 µm)

Channels = 2
Scaling (Per Pixel) = 21.11 nm X 21.11 nm X 30.00 nm
Image Size (Pixels) = 365 X 360
Image Size (Scaled) = 7.71 µm X 7.60 µm
Bit Depth = 16 Bit
Image Center Position = X: 57.77 mm, Y: 35.27 mm
Stage Position = X: 57.77 mm, Y: 35.27 mm
ROI Center Offset = X: 0.00 µm, Y: 0.00 µm

647 -

Reflectors = SR HE LBF 405/488/561/642
Beam Splitter = 405, 488, 561, 642
Filter Excitation Wavelength = 200 - 405, 200 - 488, 200 - 561, 200 - 642
Filter Emission Wavelength = 419 - 470, 503 - 546, 576 - 617, 657 - 800
Contrast Method = Fluorescence
Illumination Wavelength = 640
Channel Name = T1-Axiocam 820
Excitation Wavelength = 640
Emission Wavelength = 729
Effective NA = 1.4
Detection Wavelength = 419 - 470, 503 - 546, 576 - 617, 657 - 800
Imaging Device = Axiocam 820
Camera Adapter = 1X
Exposure Time = 100 ms
Depth of Focus = 1.13 µm
Binning Mode = 2,2
Laser Wavelength = 640 nm @ 1.0%
Frame Time = 1.33 s
Scan Direction = Unidirectional
Grating = 36.5 µm grating

488 -

Reflectors = SR HE LBF 405/488/561/642
Beam Splitter = 405, 488, 561, 642
Filter Excitation Wavelength = 200 - 405, 200 - 488, 200 - 561, 200 - 642
Filter Emission Wavelength = 419 - 470, 503 - 546, 576 - 617, 657 - 800
Contrast Method = Fluorescence
Illumination Wavelength = 488
Channel Name = T2-Axiocam 820
Excitation Wavelength = 488
Emission Wavelength = 525
Effective NA = 1.4
Detection Wavelength = 419 - 470, 503 - 546, 576 - 617, 657 - 800
Imaging Device = Axiocam 820
Camera Adapter = 1X
Exposure Time = 120 ms
Depth of Focus = 0.81 µm
Binning Mode = 2,2
Laser Wavelength = 488 nm @ 1.00%
Frame Time = 1.59 s
Scan Direction = Unidirectional
Grating = 27.5 µm grating

Post Processing - SIM Processing

Processing Dimension = 3D
Result Sampling = 4
Process Sampling = N/A
Channels = 2
Algorithm = SIM
SIM Settings = Standard
Auto Sharpness = On
Sharpness = 11.0018 (647), 11.2478 (488)
Fitting = Fast Fit
Normalization = Auto

2-Dimensional View - Panel A

Lattice SIM optical section acquired at Z-plane 48 of 95 showing Rabbit anti-Human ATM.p (Serine 1981) Recombinant Monoclonal, IgG - (BLR031P), detected using Identifyn® SRM Alexa Fluor™ 647 affinity-purified Goat Anti-Rabbit F(ab')□ (H + L) (red), and Mouse anti-Human H2Ax Monoclonal, IgG1 - (1H1D9/B7), detected using Identifyn® SRM Alexa Fluor™ 488 affinity-purified Donkey Anti-Mouse F(ab')□ (H + L) (green). A white box denotes the region of interest (ROI) selected for colocalization analysis in Panels B and C.

Colocalization View - Panels B and C

Horizontal Axis - AF647, Threshold 5707, Range Auto
Vertical Axis - AF488, Threshold 15509, Range Auto

Image Measurement = Entire Field of Panel B

Colocalization analysis of phospho-ATM (X-axis) and H2Ax (Y-axis) was performed across the entire image acquisition.

Phospho-ATM shows a lack of colocalization with H2Ax, consistent with the known biology of phospho-ATM signaling and total H2Ax distribution.

Summary

Panels B and C - Enlarged regions of interest (ROIs) from the same Lattice SIM acquisition shown in Panel A, demonstrating the spatial relationship between phospho-ATM and H2Ax following etoposide-induced DNA damage. Rabbit anti-Human ATM.p (Serine 1981) Recombinant Monoclonal, IgG - (BLR031P), detected using Identifyn® SRM Alexa Fluor™ 647 affinity-purified Goat Anti-Rabbit F(ab')□ (H + L) (red), and Mouse anti-Human H2Ax Monoclonal, IgG1 - (1H1D9/B7), detected using Identifyn® SRM Alexa Fluor™ 488 affinity-purified Donkey Anti-Mouse F(ab')□ (H + L) (green), demonstrate minimal direct signal overlap throughout the analyzed nuclear volume despite robust phospho-ATM aggregate formation and strong DNA damage-associated response.

At Lattice SIM resolution (~60-80 nm XY), the apparent broad colocalization observed in lower-resolution widefield datasets becomes substantially resolved into spatially distinct signaling territories. This finding is biologically consistent with the established role of activated phospho-ATM as an upstream DNA damage response kinase that phosphorylates H2Ax into γH2AX following DNA double-strand break induction. Because the present dataset measures total H2Ax rather than γH2AX specifically, strong molecular colocalization with phospho-ATM is not expected. Instead, phospho-ATM localizes to active checkpoint-associated signaling domains and DNA damage-responsive chromatin territories, while total H2Ax remains broadly distributed throughout the nucleosomal landscape of the nucleus.

Importantly, despite the relative absence of direct overlap, phospho-ATM exhibits a pronounced intranuclear response to etoposide treatment, forming concentrated punctate aggregates consistent with localized ATM activation and recruitment to DNA-damage-associated signaling microenvironments. The progressive loss of apparent colocalization with increasing spatial resolution strongly supports the specificity of the Identifyn® phospho-ATM antibody, as the observed localization pattern closely mirrors the known biology of ATM activation rather than nonspecific chromatin-wide staining.

Collectively, these findings demonstrate that while diffraction-limited imaging modalities can suggest strong colocalization between phospho-ATM and total H2Ax, super-resolution Lattice SIM imaging reveals that these signals largely occupy adjacent or overlapping nuclear response territories rather than identical molecular structures. This distinction underscores the importance of increasing spatial resolution within the Stepdown Methodology™ when interpreting DNA damage-associated signaling relationships and assessing the true molecular organization of repair-associated chromatin domains.

Image Correction

NONE

Image by J. H. Cheong
Image Analysis and Data Presentation by B.T. Bennett

SOURCE PROVENANCE

Catalog	PA-RR-000012
Stage	SIM
Instrument	ZEISS Elyra

SOURCE PROVENANCE

Microscope configuration	Zeiss Elyra 5 Lattice SIM, AxioObserver.Z1/ 7 using Plan-Apochromat 63X/1.40 oil DIC M27, 1X Tubelens, was used with the following parameters for each dye:
Structured source metadata values	50
Metadata source	PRESERVED_SOURCE_METHOD_PDF_TEXT
Cell model	HeLa
Image SHA-256	D7E374107F8EC8C7AFB4161EDC6A08FA929D372ED15C8A8839027600DCA30B14
Method PDF SHA-256	8FB296CEC2CB67178A298ABDA4604B6BE358A123CAD79F06F5DA2E555206DB0B

ORIGINAL IMAGE EVIDENCE / SIM²

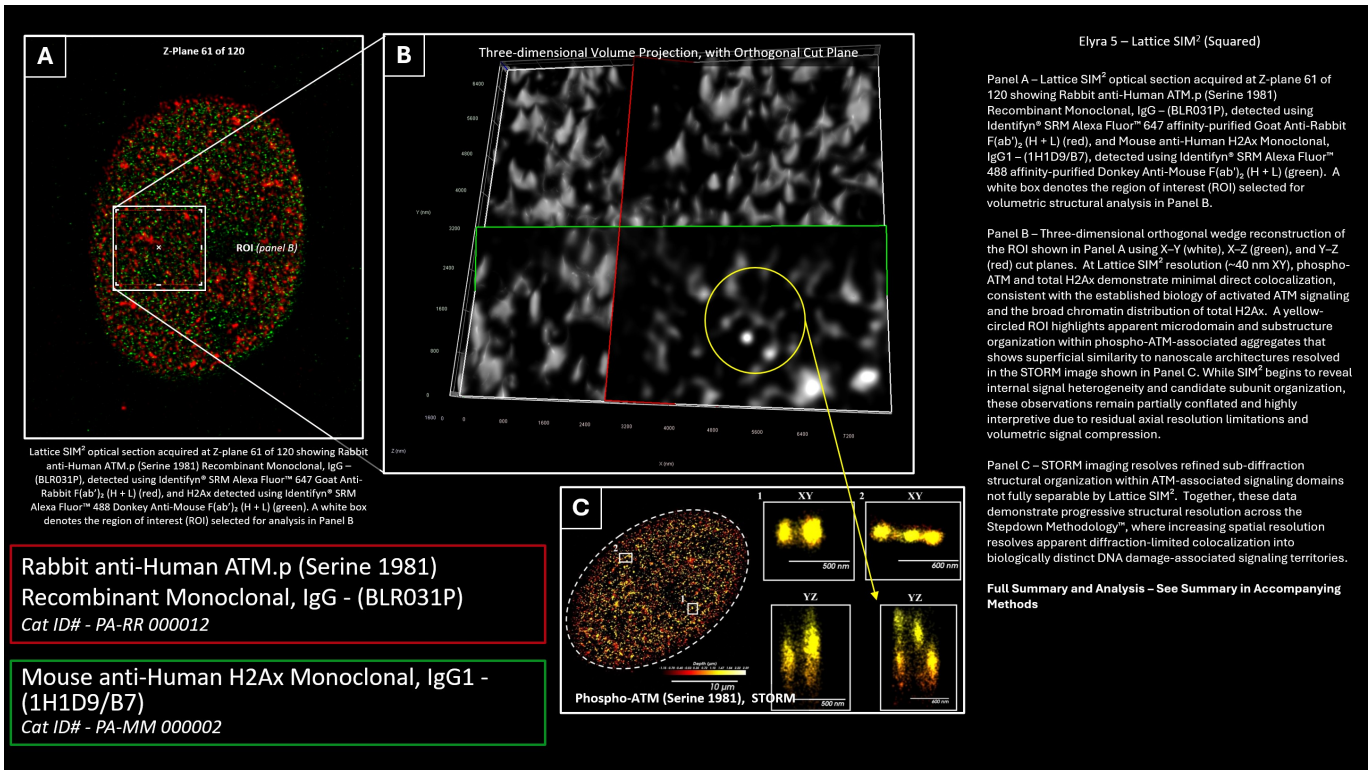

EVIDENCE TIER	SIM²
INSTRUMENT	ZEISS Elyra
CELL MODEL	HeLa
DETECTED DYES	405/DAPI; 488; 647
METADATA VALUES	63

STRUCTURED ACQUISITION METADATA / SIM²

The values below were deterministically extracted from the preserved Identifyn method PDF text. They remain source-documented metadata, not new BENNETT measurements.

FIELD	SOURCE-DOCUMENTED VALUE
Platform / configuration	Zeiss Elyra 5 Lattice SIM, AxioObserver.Z1/ 7 using Plan-Apochromat 63X/1.40 oil DIC M27, 1X Tubelens, was used with the following parameters for each dye:
Objective	Plan-Apochromat 63X/1.40 oil DIC M27
Z-Stack	120 Slices (3.57 µm)
Channels	2
Scaling (Per Pixel)	0.02111 µm X 0.02111 µm X 0.03000 µm
Image Size (Pixels)	1557 X 1805 | 376 X 330
Image Size (Scaled)	32.87 µm X 38.11 µm | 7.94 µm X 6.97 µm
Bit Depth	16 Bit
Image Center Position	X: 57.77 mm, Y: 35.27 mm
Stage Position	X: 57.77 mm, Y: 35.27 mm
ROI Center Offset	X: 0.00 µm, Y: 0.00 µm
Reflectors	SR HE LBF 405/488/561/642
Beam Splitter	405, 488, 561, 642
Filter Excitation Wavelength	200 - 405, 200 - 488, 200 - 561, 200 - 642
Filter Emission Wavelength	419 - 470, 503 - 546, 576 - 617, 657 - 800
Contrast Method	Fluorescence
Illumination Wavelength	640 | 488
Channel Name	T1-Axiocam 820 -SR | T2-Axiocam 820-SR
Excitation Wavelength	640 | 488
Emission Wavelength	729 | 525
Effective NA	1.4
Detection Wavelength	419 - 470, 503 - 546, 576 - 617, 657 - 800
Imaging Device	Axiocam 820
Camera Adapter	1X
Exposure Time	100 ms | 120 ms
Depth of Focus	1.13 µm | 0.81 µm
Binning Mode	2,2
Laser Wavelength	640 nm @ 1.0% | 488 nm @ 1.00%
Frame Time	1.33 s | 1.59 s
Scan Direction	Unidirectional
Grating	36.5 µm grating | 27.5 µm grating
Result Sampling	4
Process Sampling	4

FIELD	SOURCE-DOCUMENTED VALUE
Algorithm	SIM2
Input SNR	Low
Regularization Weight	0.0000
Iterations	3
Filter	No Filter
Fitting	Fast Fit
Normalization	Auto
3D Volume Projection	Precise
Appearance	Threshold 2% all channels, Ramp 98% all channels, Maximum 100% all channels
Background	Black
Light	Brightness 100%, Azimuth 80°, Elongation -130°, Enabled Directional Lighting, Enabled Tone Mapping
Projection	View Angle 45°, Scale Z 35%, Reverse Z-Axis NOT Selected, Stereo Anaglyph NOT Selected, Camera Separation 5% (deselected), Parallax Shift 0% (deselected)
X-Y	Activate was selected, textured opaque was chosen, and a white outline of the clipped perimeter was shown; Clip Back was selected, and Clip Front was NOT selected.
Position of Clip	-20% | -28% | 0%
Clip X	0°
Clip Z	0°
X-Z	Activate was selected, textured opaque was chosen, and a green outline of the clipped perimeter was shown; Clip Back was selected, and Clip Front was NOT selected.
Clip Y	-45°
Y-Z	Activate was selected, textured opaque was chosen, and a red outline of the clipped perimeter was shown; Clip Back was selected, and Clip Front was NOT selected.

SOURCE METHOD

The text below is carried from the preserved Identifyn source record. Typography and pagination have been normalized for this preservation dossier; scientific wording has not been editorially rewritten.

Identifyn Standards for Optical Microscopy Methods™

Identifyn® Primary Antibody

Rabbit anti-Human ATM.p (Serine 1981) Recombinant Monoclonal, IgG - (BLR031P)
Cat ID# PA-RR 000012

Mouse anti-Human H2Ax Monoclonal, IgG1 - (1H1D9/B7)
Cat ID# - PA-MM 000002

Identifyn® Secondary Antibodies

Identifyn® SRM Alexa Fluor™ 647 Affinity Purified Goat Anti-Rabbit, F(ab')□ (H + L)
Cat ID# - SA 000063

Identifyn® SRM Alexa Fluor™ 488 Affinity Purified Donkey Anti-Mouse, F(ab')□ (H + L)
Cat ID# - SA 000019

ATM (ataxia-telangiectasia mutated) is a crucial serine/threonine kinase that plays a central role in the DNA damage response (DDR), particularly in response to DNA double-strand breaks (DSBs). ATM's activation and subsequent phosphorylation cascades are essential for detecting DNA damage and initiating repair processes. Here's a detailed overview of how ATM is activated, its targets, and its role in the DDR:

Activation of ATM

In response to DNA damage, particularly DSBs, ATM is activated through a series of events:

Detection of DNA Breaks: ATM can sense DNA breaks by associating with the MRN complex (MRE11, RAD50, and NBS1). This complex recognizes DSBs, leading to ATM's recruitment to the damaged site.

Autophosphorylation: Upon detection of DNA damage, ATM autophosphorylates at serine 1981 (S1981), thereby activating it. This phosphorylation event is critical for ATM's kinase activity and its ability to phosphorylate downstream targets.

Dimer-to-Monomer Transition: In its inactive form, ATM is a dimer. It transitions to an active monomeric state upon activation, allowing it to interact with and phosphorylate various downstream proteins.

Phosphorylation Targets of ATM
Once activated, ATM phosphorylates many proteins involved in the DNA damage response, cell cycle regulation, and apoptosis. Here are some critical targets of ATM:

CHK2: ATM phosphorylates CHK2, a cell cycle checkpoint control kinase. This phosphorylation helps to halt the cell cycle, allowing time for DNA repair.

p53: ATM phosphorylates p53, activating this tumor suppressor, leading to cell cycle arrest or apoptosis if the damage is irreparable.

H2AX: ATM phosphorylates histone H2AX, forming γ-H2AX, a marker of DNA damage. This modification helps signal the presence of DSBs and recruit DNA repair machinery.

BRCA1: ATM's phosphorylation of BRCA1 is critical for homologous recombination, a key DNA repair pathway for DSBs.

NBS1: As part of the MRN complex, NBS1 phosphorylation by ATM enhances the complex's DNA repair functions.

53BP1: ATM phosphorylation of 53BP1 helps recruit this protein to sites of DSBs, thereby guiding repair pathways such as non-homologous end joining (NHEJ).

Role of ATM Phosphorylation in DNA Repair

ATM-mediated phosphorylation plays a central role in coordinating the DNA damage response:
Signal Propagation: Phosphorylation cascades initiated by ATM amplify the signal in response to DNA damage, ensuring an efficient response.

Recruitment of Repair Machinery: Phosphorylation of specific proteins helps recruit DNA repair complexes to the sites of DNA damage.

Cell Cycle Regulation: ATM activation can lead to cell cycle checkpoints, preventing cells with damaged DNA from dividing.

Apoptosis: If the DNA damage is too severe to repair, ATM's activation can lead to apoptosis, preventing the propagation of damaged cells

ATM's phosphorylation in response to DNA damage is crucial for detecting DNA double-strand breaks and coordinating the DNA damage response. By phosphorylating a range of critical proteins, ATM orchestrates a complex signaling network that facilitates DNA repair, cell cycle regulation, and apoptosis, thereby maintaining genomic stability.

Method

HeLa cells were grown on acid-etched #1.5H cover glass to ~50% confluency, DNA damage was induced by treatment with 2 µM Etoposide-spiked complete growth media for 12 hours, followed by -20 °C methanol fixation and blocking with Thermo Fisher Fish Serum Blocker (cat#37527X3). The primary antibody, Rabbit anti-Human ATM.p (Serine 1981) Recombinant Monoclonal, IgG - (BLR031P), was incubated at room temperature for 1 hour at a 1:250 dilution. Cells were washed 3X in PBS. Identifyn® SRM Alexa Fluor™ 647 Affinity Purified Goat Anti-Rabbit, F(ab')□ (H + L) was incubated at room temperature for 1 hour at a dilution of 1:1000. Cells were washed 5X in PBS.

The second primary antibody, Mouse anti-Human H2Ax Monoclonal, IgG1 - (1H1D9/B7), was then incubated for 1 hour at room temperature at a dilution of 1:250. Cells were washed 3X in PBS.
Identifyn® SRM Alexa Fluor™ 488 Affinity Purified Donkey Anti-Mouse, F(ab')□ (H + L) was incubated for 1 hour at room temperature at a dilution of 1:1000. Cells were washed 5X in PBS and mounted using ProLong™ Diamond Antifade Mountant with DAPI cat#P36962.

Microscope

Zeiss Elyra 5 Lattice SIM, AxioObserver.Z1/ 7 using Plan-Apochromat 63X/1.40 oil DIC M27, 1X Tubelens, was used with the following parameters for each dye:

Z Stack - (3D) - Panel A, Z-Plane 61 of 120

Z-Stack = 120 Slices (3.57 µm)

Channels = 2
Scaling (Per Pixel) = 21.11 nm X 21.11 nm X 30.00 nm
Image Size (Pixels) = 1557 X 1805
Image Size (Scaled) = 32.87 µm X 38.11 µm
Bit Depth = 16 Bit
Image Center Position = X: 57.77 mm, Y: 35.27 mm
Stage Position = X: 57.77 mm, Y: 35.27 mm
ROI Center Offset = X: 0.00 µm, Y: 0.00 µm

Z Stack - (3D) - 3-Dimensional Volume Projection, with Orthogonal Cut Plane

Z-Stack = 120 Slices (3.57 µm)

Channels = 2
Scaling (Per Pixel) = 21.11 nm X 21.11 nm X 30.00 nm
Image Size (Pixels) = 376 X 330
Image Size (Scaled) = 7.94 µm X 6.97 µm
Bit Depth = 16 Bit
Image Center Position = X: 57.77 mm, Y: 35.27 mm
Stage Position = X: 57.77 mm, Y: 35.27 mm
ROI Center Offset = X: 0.00 µm, Y: 0.00 µm

647 -

Reflectors = SR HE LBF 405/488/561/642
Beam Splitter = 405, 488, 561, 642
Filter Excitation Wavelength = 200 - 405, 200 - 488, 200 - 561, 200 - 642
Filter Emission Wavelength = 419 - 470, 503 - 546, 576 - 617, 657 - 800
Contrast Method = Fluorescence
Illumination Wavelength = 640
Channel Name = T1-Axiocam 820 -SR
Excitation Wavelength = 640
Emission Wavelength = 729
Effective NA = 1.4
Detection Wavelength = 419 - 470, 503 - 546, 576 - 617, 657 - 800
Imaging Device = Axiocam 820
Camera Adapter = 1X
Exposure Time = 100 ms
Depth of Focus = 1.13 µm
Binning Mode = 2,2
Laser Wavelength = 640 nm @ 1.0%
Frame Time = 1.33 s
Scan Direction = Unidirectional
Grating = 36.5 µm grating

488 -

Reflectors = SR HE LBF 405/488/561/642
Beam Splitter = 405, 488, 561, 642
Filter Excitation Wavelength = 200 - 405, 200 - 488, 200 - 561, 200 - 642
Filter Emission Wavelength = 419 - 470, 503 - 546, 576 - 617, 657 - 800
Contrast Method = Fluorescence
Illumination Wavelength = 488
Channel Name = T2-Axiocam 820-SR
Excitation Wavelength = 488
Emission Wavelength = 525
Effective NA = 1.4
Detection Wavelength = 419 - 470, 503 - 546, 576 - 617, 657 - 800
Imaging Device = Axiocam 820
Camera Adapter = 1X
Exposure Time = 120 ms
Depth of Focus = 0.81 µm
Binning Mode = 2,2
Laser Wavelength = 488 nm @ 1.00%
Frame Time = 1.59 s
Scan Direction = Unidirectional
Grating = 27.5 µm grating

Post Processing - SIM2 Processing

Processing Dimension - 3D
Result Sampling = 4
Process Sampling = 4
Channels = 2
Algorithm = SIM2
Input SNR = Low
Regularization Weight = 0.0000
Iterations = 3
Filter = No Filter
Fitting = Fast Fit
Normalization = Auto

2-Dimensional View - Panel A

Lattice SIM2 optical section acquired at Z-plane 61 of 120 showing Rabbit anti-Human ATM.p (Serine 1981) Recombinant Monoclonal, IgG - (BLR031P), detected using Identifyn® SRM Alexa Fluor™ 647 affinity-purified Goat Anti-Rabbit F(ab')□ (H + L) (red), and Mouse anti-Human H2Ax Monoclonal, IgG1 - (1H1D9/B7), detected using Identifyn® SRM Alexa Fluor™ 488 affinity-purified Donkey Anti-Mouse F(ab')□ (H + L) (green). A white box denotes the region of interest (ROI) selected for analysis in Panel B.

3D Image Processing - Panel B

3D Volume Projection = Precise
Appearance = Threshold 2% all channels, Ramp 98% all channels, Maximum 100% all channels
Background = Black
Light = Brightness 100%, Azimuth 80°, Elongation -130°, Enabled Directional Lighting, Enabled Tone Mapping
Projection = View Angle 45°, Scale Z 35%, Reverse Z-Axis NOT Selected, Stereo Anaglyph NOT Selected, Camera Separation 5% (deselected), Parallax Shift 0% (deselected)

Clipping Image Process - Panel B

Clipping planes are introduced in Panel B to highlight the phospho-ATM within the nuclear compartment by adjusting or cutting away portions of the image using a triple-wedge cut, removing parts of the image in the X-Y, X-Z, and Y-Z planes.

X-Y = Activate was selected, textured opaque was chosen, and a white outline of the clipped perimeter was shown; Clip Back was selected, and Clip Front was NOT selected.

Position of Clip = -20%
Clip X = 0°
Clip Z = 0°

X-Z = Activate was selected, textured opaque was chosen, and a green outline of the clipped perimeter was shown; Clip Back was selected, and Clip Front was NOT selected.

Position of Clip = -28%
Clip Y = -45°
Clip Z = 0°

Y-Z = Activate was selected, textured opaque was chosen, and a red outline of the clipped perimeter was shown; Clip Back was selected, and Clip Front was NOT selected.

Position of Clip = 0%
Clip Y = -45°
Clip Z = 0°

Summary

Panel A shows a Lattice SIM² optical section acquired at Z-plane 61 of 120, demonstrating phospho-ATM and H2Ax distribution following etoposide-induced DNA damage. Rabbit anti-Human ATM.p (Serine 1981) Recombinant Monoclonal, IgG - (BLR031P), detected using Identifyn® SRM Alexa Fluor™ 647 affinity-purified Goat Anti-Rabbit F(ab')□ (H + L) (red), and Mouse anti-Human H2Ax Monoclonal, IgG1 - (1H1D9/B7), detected using Identifyn® SRM Alexa Fluor™ 488 affinity-purified Donkey Anti-Mouse F(ab')□ (H + L) (green), demonstrate highly organized intranuclear redistribution following genotoxic stress. A white box denotes the region of interest selected for three-dimensional structural analysis in Panel B.

Panel B presents a three-dimensional orthogonal wedge reconstruction of the selected ROI, employing simultaneous X-Y (white), X-Z (green), and Y-Z (red) cut planes to interrogate the organization of the volumetric signal. Prior Airyscan and Lattice SIM datasets demonstrated that phospho-ATM and total H2Ax progressively lose apparent colocalization as spatial resolution increases toward ~60 nm, strongly supporting the biological specificity of the Identifyn® phospho-ATM antibody and the expected segregation of activated ATM signaling from broadly distributed total H2Ax chromatin. Within the Lattice SIM² dataset, however, the increased resolving power approaching ~40 nm

XY begins to reveal internal signal heterogeneity and apparent microdomain organization within phospho-ATM-associated aggregates.

In the lower-right orthogonal wedge reconstruction, a yellow-circled region of interest highlights structural patterns that appear superficially reminiscent of the nanoscale subunit architectures resolved by STORM imaging in Panel C. At this resolution scale, SIM² may begin to suggest the presence of subdomains, clustered repair assemblies, or partially separated signaling territories within ATM-associated DNA damage response foci. However, these observations remain highly interpretive. Even at ~40 nm XY resolution, SIM² remains limited by axial resolution constraints and residual signal convolution, such that apparent "subunits" may still represent overlapping molecular populations compressed within the diffraction volume. In contrast, STORM imaging achieves substantially higher localization precision and may be metaphorically viewed as "seeing inside" the broader volumetric signal observed in SIM².

Biologically, activated phospho-ATM functions as a master upstream kinase coordinating the DNA double-strand break response through phosphorylation-dependent checkpoint signaling, chromatin remodeling, and recruitment of downstream repair machinery, including phosphorylation of H2Ax into γH2AX. Because the present dataset measures total H2Ax rather than γH2AX specifically, direct molecular colocalization is not expected, and the observed spatial segregation is therefore biologically appropriate. Importantly, the progression from Airyscan through Lattice SIM and ultimately Lattice SIM² demonstrates the power of the Stepdown Methodology™ in progressively resolving apparent colocalization into structurally distinct DNA damage-associated signaling territories.

Nevertheless, the dataset also highlights the fundamental limitations of optical super-resolution when interrogating molecular architecture at biologically relevant scales. ATM itself is a large kinase complex, while nucleosomal and chromatin-associated signaling domains exist at dimensions approaching or below the resolving capacity of SIM². Thus, although super-resolution modalities provide increasingly valuable insights into response, redistribution, aggregate formation, and candidate spatial organization, caution is warranted when interpreting apparent microdomains or presumed molecular subunits without true nanoscale localization methods such as STORM.

Image Correction

Panel B, the 647 channel was changed from its default red to white to improve visualization of the dataset.

Image by J. H. Cheong
Image Analysis and Data Presentation by B.T. Bennett

SOURCE PROVENANCE

Catalog	PA-RR-000012
Stage	SIM²
Instrument	ZEISS Elyra
Microscope configuration	Zeiss Elyra 5 Lattice SIM, AxioObserver.Z1/ 7 using Plan-Apochromat 63X/1.40 oil DIC M27, 1X Tubelens, was used with the following parameters for each dye:
Structured source metadata values	63
Metadata source	PRESERVED_SOURCE_METHOD_PDF_TEXT
Cell model	HeLa
Image SHA-256	34D26570A1A58ECD7FF6BB10DE5BDF63183E0356B40B92C7DF95ECA1E4269EE1

SOURCE PROVENANCE

Method PDF SHA-256	7442BC9DFA9199673B41CD107549FB95CBF242F0B5D7F7A3C065E66997A15B0C

ORIGINAL IMAGE EVIDENCE / SINGLE-MOLECULE STORM

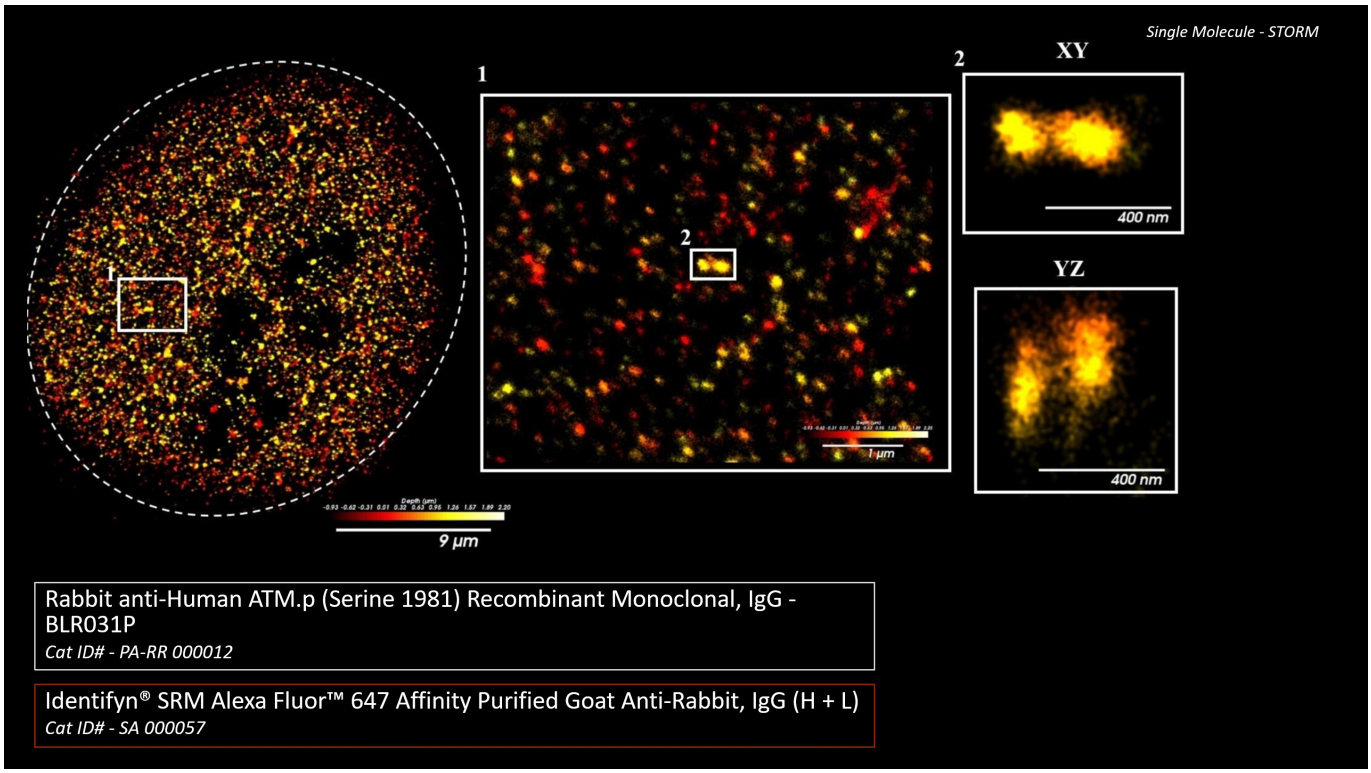

EVIDENCE TIER	Single-molecule STORM
INSTRUMENT	Bruker Vutara VXL
CELL MODEL	HeLa
DETECTED DYES	647
METADATA VALUES	80

STRUCTURED ACQUISITION METADATA / SINGLE-MOLECULE STORM

The values below were deterministically extracted from the preserved Identifyn method PDF text. They remain source-documented metadata, not new BENNETT measurements.

FIELD	SOURCE-DOCUMENTED VALUE
Platform / configuration	Bruker Vutara VXL Biplane Single Molecule Microscope, using an Olympus 60x/1.30 Silicon Oil objective, was used with the following parameters:
Objective	Olympus 60x/1.30 Silicon Oil objective
Number of Probes	1
Number of Simultaneous Probes	1
Number of Reference Probes	1
Camera	Both Cameras
Color Channel	Both Channels
Probe Capture Mode	Interleaved
Z -Stack Capture Mode	Interleaved
Multiple Location Capture	Not selected
Post Record Reference	Not Selected
Fluidics	Not Selected
Autofocus Drift Correction	On
Biplane Module	635 nm Dichroic
Objective	Silicon Selected
Stage Insert	Rectangular Selected
Coarse Focus Position	8-Well Chamber Selected
Dichroic	SuperRes
PSF	(Red, Orange)
Heater	Current: 26
Recording Vertical Field of View	100%
Widefield Camera Exposure Time	100 ms | 20 ms
Super Resolution Camera Exposure Time	20 ms
Widefield Camera Binning	1
Per-Probe Exposure Time	Selected
Predefined Probe	First probe: 640 nm (635 nm Dichroic); First reference probe: 640 nm (635 nm Dichroic)
Photoactivation/Imaging Laser	0% Selected
Exposure Time	20 ms Selected
Record Workflow	Selected Options
View Mode	Widefield 200 µm
Capture Mode	Live
Piezo Current	183.4 µm

FIELD	SOURCE-DOCUMENTED VALUE
Widefield 640 nm	0.1X Neutral Density Filter: Selected, @ 0.2% Laser Input
Reference Probe 1 Laser control 640 nm (635 nm Dichroic)	Not Selected
Widefield camera Exposure Time	100 ms
Widefield Laser	"Widefield 640 nm" was deselected, and "calibrate" under Autofocus was selected.
Current Position	-0.979
Current Intensity	4.5
Calibration Value	-5070 nm/unit
Autofocus Mode	Pre-Capture
SuperRes	50 µm is selected
Cell(s) or Cellular Structure Localization	Positioning of the target Cell or Subsection of the Target Cell is optimized and focused.
Piezo Record	Begin: 182; End: 183.4
SuperRes 640 nm	0.1X Neutral Density Filter: Selected, @ 0.02% Laser Input
Record Workflow - Record Tab	Capture Parameters
Frames	Probe 1: 200
Z Positions	7
Cycles	20
Time Points	1
Pause Between Cycles	Not Selected
Automatic Photoactivation Laser Control	Not Selected
Laser Power	90
Cutout Width	16 px
Max Frame Accumulation	1 frame
Max Accumulation Offset	1 px
Fiducial at Max Accumulation	Not selected
Max Particles Per Frame	No Max
Background SLPE Removal	Not Selected
Cutout/Background Removal	Not Selected
Preview Cutout Positions	Selected
Probe1	BG threshold: 20
Sizing Mode	Radial Precision
Particle size	4 nm
Color by	Depth
Color Table	Single
Opacity Mode	Depth; Opacity 1: 0.1
Front-to-back Attenuation	Not Selected

FIELD	SOURCE-DOCUMENTED VALUE
Method	Particle (direct)
Time Intervals	8 Intervals
Pixel Size	50 nm
Smoothing	8.00
Radial precision	30
Axial precision	65
Clustering Algorithm	DBSCAN
Maximum Particle Distance	0.1 µm
Maximum Particle Count to Form Cluster	10
Compute Hulls	Not Selected
Compute Density Isosurfaces	Not Selected
Edit Settings	All Probes
Compute	Selected
Following Cluster Analysis Computation, under the Results Tab, ID Unassigned	Deselected

SOURCE METHOD

The text below is carried from the preserved Identifyn source record. Typography and pagination have been normalized for this preservation dossier; scientific wording has not been editorially rewritten.

Identifyn Standards for Optical Microscopy Methods™

Identifyn® Primary Antibody

Rabbit anti-Human ATM.p (Serine 1981) Recombinant Monoclonal, IgG - (BLR031P)
Cat ID# - PA-RR 000012

Identifyn® Secondary Antibody

Identifyn® SRM Alexa Fluor™ 647 Affinity Purified Goat Anti-Rabbit, IgG (H + L)
Cat ID# - SA 000057

ATM (ataxia-telangiectasia mutated) is a crucial serine/threonine kinase that plays a central role in the DNA damage response (DDR), particularly in response to DNA double-strand breaks (DSBs). ATM's activation and subsequent phosphorylation cascades are essential for detecting DNA damage and initiating repair processes. Here's a detailed overview of how ATM is activated, its targets, and its role in the DDR:

Activation of ATM

In response to DNA damage, particularly DSBs, ATM is activated through a series of events:
Detection of DNA Breaks: ATM can sense DNA breaks by associating with the MRN complex (MRE11, RAD50, and NBS1). This complex recognizes DSBs, leading to ATM's recruitment to the damaged site.

Autophosphorylation: Upon detection of DNA damage, ATM autophosphorylates at serine 1981 (S1981), thereby activating it. This phosphorylation event is critical for ATM's kinase activity and its ability to phosphorylate downstream targets.

Dimer-to-Monomer Transition: In its inactive form, ATM is a dimer. It transitions to an active monomeric state upon activation, allowing it to interact with and phosphorylate various downstream proteins.

Phosphorylation Targets of ATM
Once activated, ATM phosphorylates many proteins involved in the DNA damage response, cell cycle regulation, and apoptosis. Here are some critical targets of ATM:

CHK2: ATM phosphorylates CHK2, a cell cycle checkpoint control kinase. This phosphorylation helps to halt the cell cycle, allowing time for DNA repair.

p53: ATM phosphorylates p53, activating this tumor suppressor, leading to cell cycle arrest or apoptosis if the damage is irreparable.

H2AX: ATM phosphorylates histone H2AX, forming γ-H2AX, a marker of DNA damage. This modification signals the presence of DSBs and recruits DNA repair machinery.

BRCA1: ATM's phosphorylation of BRCA1 is critical for homologous recombination, a key DNA repair pathway for DSBs.

NBS1: As part of the MRN complex, NBS1 phosphorylation by ATM enhances the complex's DNA repair functions.

53BP1: ATM phosphorylation of 53BP1 helps recruit this protein to sites of DSBs, thereby guiding repair pathways such as non-homologous end joining (NHEJ).

Role of ATM Phosphorylation in DNA Repair

ATM-mediated phosphorylation plays a central role in coordinating the DNA damage response:
Signal Propagation: Phosphorylation cascades initiated by ATM amplify the signal in response to DNA damage, ensuring an efficient response.

Recruitment of Repair Machinery: Phosphorylation of specific proteins helps recruit DNA repair complexes to the sites of DNA damage.

Cell Cycle Regulation: ATM activation can lead to cell cycle checkpoints, preventing cells with damaged DNA from dividing.

Apoptosis: If the DNA damage is too severe to repair, ATM's activation can lead to apoptosis, preventing the propagation of damaged cells

ATM's phosphorylation in response to DNA damage is crucial for detecting DNA double-strand breaks and coordinating the DNA damage response. By phosphorylating a range of critical proteins, ATM orchestrates a complex network of signaling events that facilitate DNA repair, cell cycle regulation, and apoptosis, thereby maintaining genomic stability.

Method

HeLa cells were grown in a µ-Slide 8 Well high-Glass Bottom Ibidi chamber. DNA damage was induced via treatment with 2 µM etoposide-spiked complete growth media for 12 hours, followed by -20 °C methanol fixation and blocked with Thermo Fisher Fish Serum Blocker cat#37527X3. The primary antibody, Rabbit anti-Human ATM.p (Serine 1981) Recombinant Monoclonal, IgG was incubated for 1 hour at room temperature at a dilution of 1:100. Cells were washed 3X in Identifyn®'s proprietary Wash Buffer, and Identifyn® SRM Alexa Fluor™ 647 Affinity Purified Goat Anti-Rabbit, IgG (H + L) was incubated at room temperature for 1 hour at a dilution of 1:200. Cells were washed 5 times in Identifyn®'s proprietary Wash Buffer followed by the addition of Identifyn®'s proprietary STORM Buffer to the sample chamber enabling image acquisition.

Microscope

Bruker Vutara VXL Biplane Single Molecule Microscope, using an Olympus 60x/1.30 Silicon Oil objective, was used with the following parameters:

Calibration -

Calibration follows Identifyn®'s Calibration Standard Operating Procedure, which can be found here.

https://identifyn.com/storm-calibration

Image Acquisition -

SRX Software - Under the 'Single Molecule Localization' tab, 'Record' is selected and contains the following workflow tabs and parameters.

Configuration Tab - Capture Configuration

Number of Probes: 1
Number of Simultaneous Probes: 1
Number of Reference Probes: 1
Camera: Both Cameras
Color Channel: Both Channels
Probe Capture Mode: Interleaved
Z -Stack Capture Mode: Interleaved
Multiple Location Capture: Not selected
Post Record Reference: Not Selected
Fluidics: Not Selected
Autofocus Drift Correction: On

Microscope configuration

Biplane Module: 635 nm Dichroic
Objective: Silicon Selected
Stage Insert: Rectangular Selected
Coarse Focus Position: 8-Well Chamber Selected
Dichroic: SuperRes
PSF: (Red, Orange)
Heater: Current: 26

Camera Configuration

Recording Vertical Field of View: 100%
Widefield Camera Exposure Time: 100 ms
Super Resolution Camera Exposure Time: 20 ms
Widefield Camera Binning: 1
Per-Probe Exposure Time: Selected

Probe Configuration

Predefined Probe: First probe: 640 nm (635 nm Dichroic); First reference probe: 640 nm (635 nm Dichroic)
Photoactivation/Imaging Laser: 0% Selected
Exposure Time: 20 ms Selected

Experiment Configuration

Record Workflow: Selected Options
View Mode: Widefield 200 µm
Capture Mode: Live

Stage and Piezo Selection

Examination of the Sample

Cell(s) or Cellular Structure Localization - The red-bordered box identifies the area of the SuperRes view and defines a suitable cell(s) or cellular structure. The cell(s) or structures are optimally focused.

Piezo Current: 183.4 µm

Probe 1 Laser control 640 nm (635 nm Dichroic)

Widefield 640 nm: 0.1X Neutral Density Filter: Selected, @ 0.2% Laser Input
Reference Probe 1 Laser control 640 nm (635 nm Dichroic): Not Selected

Advanced Tools Option

Widefield camera Exposure Time: 100 ms
Default values are maintained unless otherwise noted.

Widefield Laser: "Widefield 640 nm" was deselected, and "calibrate" under Autofocus was selected.

Autofocus - Calibration Values

Current Position: -0.979
Current Intensity: 4.5
Calibration Value: -5070 nm/unit
Autofocus Mode: Pre-Capture

View Mode

SuperRes: 50 µm is selected

Capture Mode

Live

Stage and Piezo Selection

Cell(s) or Cellular Structure Localization: Positioning of the target Cell or Subsection of the Target Cell is optimized and focused.

Piezo Record: Begin: 182; End: 183.4

Probe 1 Laser control 640 nm (635 nm Dichroic)

SuperRes 640 nm: 0.1X Neutral Density Filter: Selected, @ 0.02% Laser Input

Reference Probe 1 Laser control 640 nm (635 nm Dichroic)

Not Selected

Advanced Tools

Widefield Camera Exposure Time: 20 ms
Default values are maintained unless otherwise noted.

Record Workflow - Record Tab: Capture Parameters

Frames: Probe 1: 200
Z Positions: 7
Cycles: 20
Time Points: 1
Pause Between Cycles: Not Selected
Automatic Photoactivation Laser Control: Not Selected

Probe 1 Laser control 640 nm (635 nm Dichroic)

Laser Power: 90

Expert Configuration Options - The Localization Tab

Beyond the values shown, all other parameters were set to default values.

Localization

Cutout Width: 16 px
Max Frame Accumulation: 1 frame
Max Accumulation Offset: 1 px
Fiducial at Max Accumulation: Not selected
Max Particles Per Frame: No Max
Background SLPE Removal: Not Selected
Cutout/Background Removal: Not Selected
Preview Cutout Positions: Selected

Record Workflow - Localization Tab

Data Collection

The folder is created automatically with the localization file for this image acquisition.

Recording Summary

All parameters were carried over from previous tabs and are kept except:

Probe1: BG threshold: 20

Region of Interest -

Not selected

Display -

Was deployed to inspect if the BG threshold applied chooses localizations in an expected manner

Record Workflow - View Tab

Region of Interest

Default values

Visualization Parameters

Point Splatting
Sizing Mode: Radial Precision
Particle size: 4 nm
Color by: Depth
Color Table: Single
Opacity Mode: Depth; Opacity 1: 0.1
Front-to-back Attenuation: Not Selected

Post Acquisition analysis - View Tab

Drift Correction - Computed with the following parameters:

Method: Particle (direct)
Time Intervals: 8 Intervals
Pixel Size: 50 nm
Smoothing: 8.00

Advanced Particle Filters - Applied to the drift-corrected data with the following parameters

Radial precision: 30
Axial precision: 65

The other parameters were not applied.

Statistical Analysis - Computed to clean low background signals.

Statistics Dialog - Cluster Analysis

Clustering Algorithm: DBSCAN

Parameters

Maximum Particle Distance: 0.1 μm
Maximum Particle Count to Form Cluster: 10
Compute Hulls: Not Selected
Compute Density Isosurfaces: Not Selected
Edit Settings: All Probes
Compute: Selected
Following Cluster Analysis Computation, under the Results Tab, ID Unassigned: Deselected

---

Image by P. Raut

SOURCE PROVENANCE

Catalog	PA-RR-000012
Stage	Single-molecule STORM
Instrument	Bruker Vutara VXL
Microscope configuration	Bruker Vutara VXL Biplane Single Molecule Microscope, using an Olympus 60x/1.30 Silicon Oil objective, was used with the following parameters:
Structured source metadata values	80
Metadata source	PRESERVED_SOURCE_METHOD_PDF_TEXT
Cell model	HeLa
Image SHA-256	0925FDD8B2CD9AB95AE04CF736F76755EE879E3A1890B129D46090CA1A5AD865
Method PDF SHA-256	1EF362B1B982F356DF2A5FE2C80F330F72ADDAC99F5698A2AD1C3BE04F596AD0

ORIGINAL IMAGE EVIDENCE / CONTROL

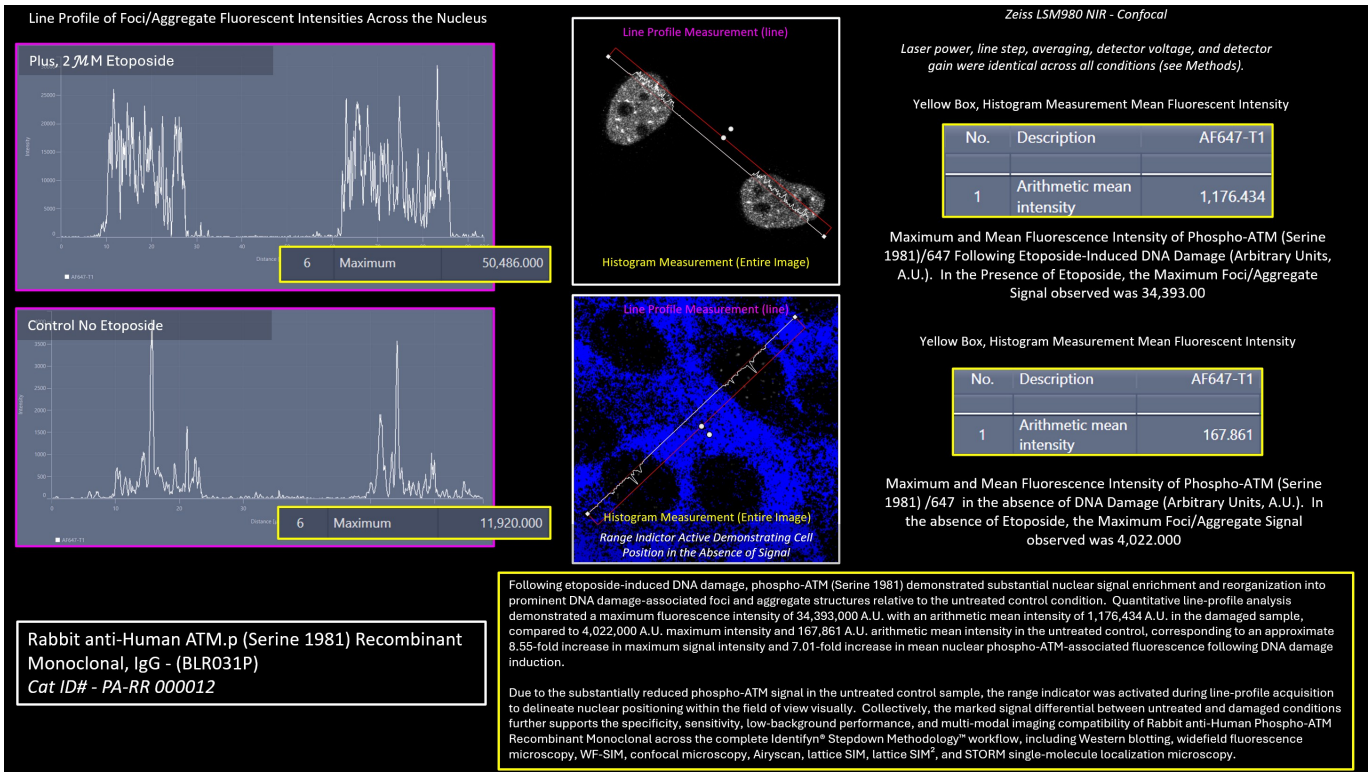

EVIDENCE TIER	Control
INSTRUMENT	Not stated
CELL MODEL	HeLa
DETECTED DYES	405/DAPI; 488; 647
METADATA VALUES	53

STRUCTURED ACQUISITION METADATA / CONTROL

The values below were deterministically extracted from the preserved Identifyn method PDF text. They remain source-documented metadata, not new BENNETT measurements.

FIELD	SOURCE-DOCUMENTED VALUE
Platform / configuration	Not stated
Z-Stack	73 Slices (2.16 µm)
Channels	1
Scaling (Per Pixel)	0.059 µm X 0.059 µm X 0.030 µm | 0.059 µm X 0.059 µm
Image size (Pixels)	1341 X 1115 | 1066 X 1066
Image Size (Scaled)	78.85 µm X 65.56 µm | 62.72 µm X 62.72 µm
Bit Depth	16 Bit
Image Center Position	X: 97.20 mm, Y: 46.14 mm | X: 70.58 mm, Y: 54.20 mm
Stage Position	X: 97.20 mm, Y: 46.14 mm | X: 70.58 mm, Y: 54.20 mm
ROI Center Offset	X: 0.00 µm, Y: 0.00 µm
Reflector	None
Contrast Method	Fluorescence
Pinhole	1.00 AU / 65 µm
LMS MBS	MBS 488/639 & 405/730
LMS SBS	SBS SP 615
Laser Wavelength	639 nm @ 0.3%
Laser Blanking	Enabled
Scan Mode	Frame
Scan Zoom	1.5 | 2.1
Rotation	0°
Sampling	1.20
Pixel Time	0.26 µs | 0.32 µs
Frame Time	5.63 s | 3.52 s
LSM Scan Speed	11
Scan Direction	Bidirectional
Line Step	1
Averaging	8
Excitation Wavelength	653
Emission Wavelength	668
Effective NA	1.4
Detection Wavelength	640 - 732
Imaging Device	GaAsP-Pmt3
Detector Type	GaAsP-PMT
Detector Gain	500 V

FIELD	SOURCE-DOCUMENTED VALUE
Detector Offset	0
Detector Digital Gain	1.0
LSM Plus Mode	Filter: 8.1 (3D, Auto) | Filter: 6.2 (3D, Auto)
Profile Definition	Stroke Thickness 1.00, Normal View, Grid Distance 1
Profile View	X and Y axes were set to Auto - X (Min 0.0 and Max 93.6), Y (Min 0.0 and Max 36113) | X and Y axes were set to Auto - X (Min 0.0 and Max 67.6), Y (Min 0.0 and Max 42444)
Histogram Definition	Normal, Histo Table set to Frequency, Bin Count 256, Bin Size was 256, Lower Threshold 0, Upper Threshold 65535
Histogram View	X and Y axes were set to Auto - X (Min 0.0 and Max 65535), Y (Min 0 and Max 2000000) | X and Y axes were set to Auto - X (Min 0.0 and Max 65535), Y (Min 0 and Max 1000000)
Arithmetic Mean intensity	1,176.434 | 167.861

SOURCE METHOD

The text below is carried from the preserved Identifyn source record. Typography and pagination have been normalized for this preservation dossier; scientific wording has not been editorially rewritten.

Identifyn Standards for Optical Microscopy Methods™

Identifyn® Primary Antibody

Rabbit anti-Human ATM.p (Serine 1981) Recombinant Monoclonal, IgG - (BLR031P)
Cat ID# PA-RR 000012

Identifyn® Secondary Antibodies

Identifyn® SRM Alexa Fluor™ 647 Affinity Purified Goat Anti-Rabbit, F(ab')□ (H + L)
Cat ID# - SA 000063

ATM (ataxia-telangiectasia mutated) is a crucial serine/threonine kinase that plays a central role in the DNA damage response (DDR), particularly in response to DNA double-strand breaks (DSBs). ATM's activation and subsequent phosphorylation cascades are essential for detecting DNA damage and initiating repair processes. Here's a detailed overview of how ATM is activated, its targets, and its role in the DDR:

Activation of ATM

In response to DNA damage, particularly DSBs, ATM is activated through a series of events:

Detection of DNA Breaks: ATM can sense DNA breaks by associating with the MRN complex (MRE11, RAD50, and NBS1). This complex recognizes DSBs, leading to ATM's recruitment to the damaged site.

Autophosphorylation: Upon detection of DNA damage, ATM autophosphorylates at serine 1981 (S1981), thereby activating it. This phosphorylation event is critical for ATM's kinase activity and its ability to phosphorylate downstream targets.

Dimer-to-Monomer Transition: In its inactive form, ATM is a dimer. It transitions to an active monomeric state upon activation, allowing it to interact with and phosphorylate various downstream proteins.

Phosphorylation Targets of ATM
Once activated, ATM phosphorylates many proteins involved in the DNA damage response, cell cycle regulation, and apoptosis. Here are some critical targets of ATM:

CHK2: ATM phosphorylates CHK2, a cell cycle checkpoint control kinase. This phosphorylation helps to halt the cell cycle, allowing time for DNA repair.

p53: ATM phosphorylates p53, activating this tumor suppressor, leading to cell cycle arrest or apoptosis if the damage is irreparable.

H2AX: ATM phosphorylates histone H2AX, forming γ-H2AX, a marker of DNA damage. This modification helps signal the presence of DSBs and recruit DNA repair machinery.

BRCA1: ATM's phosphorylation of BRCA1 is critical for homologous recombination, a key DNA repair pathway for DSBs.

NBS1: As part of the MRN complex, NBS1 phosphorylation by ATM enhances the complex's DNA repair functions.

53BP1: ATM phosphorylation of 53BP1 helps recruit this protein to sites of DSBs, thereby guiding repair pathways such as non-homologous end joining (NHEJ).

Role of ATM Phosphorylation in DNA Repair

ATM-mediated phosphorylation plays a central role in coordinating the DNA damage response:
Signal Propagation: Phosphorylation cascades initiated by ATM amplify the signal in response to DNA damage, ensuring an efficient response.

Recruitment of Repair Machinery: Phosphorylation of specific proteins helps recruit DNA repair complexes to the sites of DNA damage.

Cell Cycle Regulation: ATM activation can lead to cell cycle checkpoints, preventing cells with damaged DNA from dividing.

Apoptosis: If the DNA damage is too severe to repair, ATM's activation can lead to apoptosis, preventing the propagation of damaged cells

ATM's phosphorylation in response to DNA damage is crucial for detecting DNA double-strand breaks and coordinating the DNA damage response. By phosphorylating a range of critical proteins, ATM orchestrates a complex signaling network that facilitates DNA repair, cell cycle regulation, and apoptosis, thereby maintaining genomic stability.

Method

Plus Damage -

HeLa cells were grown on acid-etched #1.5H cover glass to ~50% confluency, DNA damage was induced by treatment with 2 µM Etoposide-spiked complete growth media for 12 hours, followed by -20 °C methanol fixation and blocking with Thermo Fisher Fish Serum Blocker (cat#37527X3). The primary antibody, Rabbit anti-Human ATM.p (Serine 1981) Recombinant Monoclonal, IgG - (BLR031P), was incubated at room temperature for 1 hour at a 1:250 dilution. Cells were washed 3X in PBS. Identifyn® SRM Alexa Fluor™ 647 Affinity Purified Goat Anti-Rabbit, F(ab')□ (H + L) was incubated at room temperature for 1 hour at a dilution of 1:1000. Cells were washed 5X in PBS.

Minus Damage -

HeLa cells were grown on acid-etched #1.5H cover glass to ~50% confluency, then fixed in -20 °C methanol and blocked with Thermo Fisher Fish Serum Blocker (cat#37527X3). The primary antibody, Rabbit anti-Human ATM.p (Serine 1981) Recombinant Monoclonal, IgG - (BLR031P), was incubated at room temperature for 1 hour at a 1:250 dilution. Cells were washed 3X in PBS.
Identifyn® SRM Alexa Fluor™ 647 Affinity Purified Goat Anti-Rabbit, F(ab')□ (H + L) was incubated at room temperature for 1 hour at a dilution of 1:1000. Cells were washed 5X in PBS and mounted using ProLong™ Diamond Antifade Mountant with DAPI (cat# P36962).

Z Stack - (3D) - Panel A, Showing Z-Plane 33 of 73

Z-Stack = 73 Slices (2.16 µm)

Channels = 1
Scaling (Per Pixel) = 0.059 µm X 0.059 µm X 0.030 µm
Image size (Pixels) = 1341 X 1115
Image Size (Scaled) = 78.85 µm X 65.56 µm
Bit Depth = 16 Bit
Image Center Position = X: 97.20 mm, Y: 46.14 mm
Stage Position = X: 97.20 mm, Y: 46.14 mm
ROI Center Offset = X: 0.00 µm, Y: 0.00 µm

Single Plane (2D)

Channels = 1
Scaling (Per Pixel) = 0.059 µm X 0.059 µm
Image size (Pixels) = 1066 X 1066
Image Size (Scaled) = 62.72 µm X 62.72 µm
Bit Depth = 16 Bit
Image Center Position = X: 70.58 mm, Y: 54.20 mm
Stage Position = X: 70.58 mm, Y: 54.20 mm
ROI Center Offset = X: 0.00 µm, Y: 0.00 µm

647 - Plus Etoposide, Upper Panel
Reflector = None
Contrast Method = Fluorescence
Pinhole = 1.00 AU / 65 µm
LMS MBS = MBS 488/639 & 405/730
LMS SBS = SBS SP 615
Laser Wavelength = 639 nm @ 0.3%
Laser Blanking = Enabled
Scan Mode = Frame
Scan Zoom = 1.5
Rotation = 0°
Sampling = 1.20
Pixel Time = 0.26 µs
Frame Time = 5.63 s
LSM Scan Speed = 11
Scan Direction = Bidirectional
Line Step = 1
Averaging = 8
Excitation Wavelength = 653
Emission Wavelength = 668
Effective NA = 1.4
Detection Wavelength = 640 - 732
Imaging Device = GaAsP-Pmt3
Detector Type = GaAsP-PMT
Detector Gain = 500 V
Detector Offset = 0
Detector Digital Gain = 1.0
LSM Plus Mode = Filter: 8.1 (3D, Auto)

647 - No Etoposide, Lower Panel - Control
Reflector = None
Contrast Method = Fluorescence
Pinhole = 1.00 AU / 65 µm
LMS MBS = MBS 488/639 & 405/730
LMS SBS = SBS SP 615
Laser Wavelength = 639 nm @ 0.3%
Laser Blanking = Enabled
Scan Mode = Frame
Scan Zoom = 2.1

Rotation = 0°
Sampling = 1.20
Pixel Time = 0.32 µs
Frame Time = 3.52 s
LSM Scan Speed = 11
Scan Direction = Bidirectional
Line Step = 1
Averaging = 8
Excitation Wavelength = 653
Emission Wavelength = 668
Effective NA = 1.4
Detection Wavelength = 640 - 732
Imaging Device = GaAsP-Pmt3
Detector Type = GaAsP-PMT
Detector Gain = 500 V
Detector Offset = 0
Detector Digital Gain = 1.0
LSM Plus Mode = Filter: 6.2 (3D, Auto)

Profile View Display - Plus DNA Damage, Top

Profile Definition = Stroke Thickness 1.00, Normal View, Grid Distance 1

Profile View = X and Y axes were set to Auto - X (Min 0.0 and Max 93.6), Y (Min 0.0 and Max 36113)

This panel measures Phospho-ATM DNA damage-induced foci/aggregates across an arbitrary line, noting that the foci/aggregate signal reached approximately ~30K A.U. at its maximum.

Measured at the Z-plane, 33 of 73.

Profile View Display - Minus DNA Damage, Bottom

Profile Definition = Stroke Thickness 1.00, Normal View, Grid Distance 1

Profile View = X and Y axes were set to Auto - X (Min 0.0 and Max 67.6), Y (Min 0.0 and Max 42444)

This panel measures Phospho-ATM in the absence of DNA damage across an arbitrary line, noting that the foci/aggregate signal reached approximately ~4K A.U. at its maximum.

Two-dimensional single plane acquisition.

Histogram Display - Plus DNA Damage, Top

Histogram Definition = Normal, Histo Table set to Frequency, Bin Count 256, Bin Size was 256, Lower Threshold 0, Upper Threshold 65535

Histogram View = X and Y axes were set to Auto - X (Min 0.0 and Max 65535), Y (Min 0 and Max 2000000)

Arithmetic Mean intensity = 1,176.434

The histogram was generated from the entire image field to quantify the overall Phospho-ATM response following DNA-damage induction. This measurement provides additional support for the observed increase in signal relative to the control condition, complementing the line-profile analysis presented alongside it.

Histogram Display - Minus DNA Damage, Bottom

Histogram Definition = Normal, Histo Table set to Frequency, Bin Count 256, Bin Size was 256, Lower Threshold 0, Upper Threshold 65535

Histogram View = X and Y axes were set to Auto - X (Min 0.0 and Max 65535), Y (Min 0 and Max 1000000)

Arithmetic Mean intensity = 167.861

The histogram was generated from the entire image field to quantify the overall Phospho-ATM protein in the absence of DNA-damage induction. This measurement provides additional support for the observed increase in signal relative to the control condition, complementing the line-profile analysis presented alongside it.

Summary

Following etoposide-induced DNA damage, Rabbit anti-Human ATM.p (Serine 1981) Recombinant Monoclonal, IgG - (BLR031P) exhibited substantial enrichment of nuclear signal and reorganization into prominent DNA damage-associated semi-resolved aggregate structures relative to the untreated control. Quantitative fluorescence intensity analysis of the damaged sample demonstrated a maximum foci/aggregate line-profile intensity of 34,393.000 A.U. with an arithmetic mean intensity of 1,176.434 A.U. In contrast, the undamaged control sample demonstrated a substantially lower maximum peak intensity of 4,022.000 A.U. and an arithmetic mean intensity of 167.861 A.U. Collectively, these measurements correspond to an approximate 8.55-fold increase in maximum phospho-ATM-associated fluorescence intensity and an approximate 7.01-fold increase in mean nuclear phospho-ATM-associated signal following etoposide-induced DNA damage, supporting significant phospho-ATM-associated signal enrichment following DNA damage induction.

In undamaged cells, the phospho-ATM signal remained comparatively diffuse and low intensity throughout the nucleus, consistent with basal ATM phosphorylation levels under non-stressed cellular conditions. Due to the minimal fluorescence signal in the untreated control sample, the range indicator was activated during line-profile acquisition to identify and visually delineate nuclear positions within the field of view. Without this positional reference, the nuclei would have been difficult to visually distinguish within the line-profile representation due to the substantially reduced phospho-ATM-associated fluorescence signal.

Importantly, the dramatic contrast observed between untreated and DNA-damaged conditions further reinforces the specificity, sensitivity, and imaging robustness of the Rabbit anti-Human ATM.p (Serine 1981) Recombinant Monoclonal antibody across the complete Identifyn® Stepdown Methodology™ workflow. Consistent localization behavior, low-background nuclear specificity, strong fluorescence intensity preservation, and reproducible foci-associated signal enrichment were maintained across widefield fluorescence microscopy, widefield structured illumination microscopy (WF-SIM), confocal microscopy, Airyscan super-resolution microscopy, lattice SIM, lattice SIM², and STORM single-molecule localization microscopy datasets. Collectively, the ability to preserve biologically coherent signal architecture and maintain compatibility across progressively demanding imaging modalities strongly supports both the performance of the phospho-ATM antibody itself and the broader validity of the Identifyn® multi-modal validation framework.

Image Correction

The phospho-ATM channel (647) was displayed in grayscale to enhance visual contrast.

Image by J.K. Bennett
Image Analysis and Data Presentation by B.T. Bennett

SOURCE PROVENANCE

Catalog	PA-RR-000012
Stage	Control
Instrument	Not stated in extracted metadata
Microscope configuration	Not stated in extracted metadata
Structured source metadata values	53
Metadata source	PRESERVED_SOURCE_METHOD_PDF_TEXT
Cell model	HeLa
Image SHA-256	65E2D61603F8AE9980180441C0AD8583A716F159F96654BA651A77AC268E6D23
Method PDF SHA-256	686FAEFA9FE70F50AE1CE23CDAA940FDCC9B6C44BA3DAF6628EC4A686EF75A39